Report No.: NM99MSC-07.2

RESEARCH

EVALUATION OF A MECHANICAL STIFFNESS GAUGE FOR COMPACTION CONTROL OF GRANULAR MEDIA

Prepared by:
Lary R. Lenke,
R. Gordon McKeen,
Matt Grush
ATR Institute
University of New Mexico

Prepared for:
New Mexico State Highway &
Transportation Department
Research Bureau

In Cooperation with:
The U.S. Department of Transportation
Federal Highway Administration

December 2001

New Mexico State Highway & Transportation Department
Research Bureau
7500 East Frontage Road
P.O. Box 94690
Albuquerque, NM 87199-4690

1. Report No.	2. Government Accession No.	3. Recipient's Catalog No.
NM99MSC-07.2		

4. Title and Subtitle	5. Report Date
Evaluation of a Mechanical Stiffness Gauge for Compaction Control of Granular Media	December 2001
	6. Performing Organization Code

7. Author(s)	8. Performing Organization Report No.
Lary R. Lenke, R. Gordon McKeen, Matt Grush	

9. Performing Organization Name and Address	10. Work Unit No. (TRAIS)
ATR Institute University of New Mexico 1001 University Blvd., SE, Suite 103 Albuquerque, NM 87106	11. Contract or Grant No. CO 3924

12. Sponsoring Agency Name and Address	13. Type of Report and Period Covered
Research Bureau New Mexico State Highway & Transportation Department 7500 East Frontage Road P.O. Box 94690 Albuquerque, NM 87199-4690	Final Report June 1999 - December 2001
	14. Sponsoring Agency Code

15. Supplementary Notes

David Albright, NMSH&TD Research Bureau Chief; Rais Rizvi, NMSH&TD Research Engineer; Stan Matingly, FHWA Research & Technology Engineer; Steve Von Stein, FHWA Pavement Engineer.

16. Abstract

The use of nuclear methods for compaction control is increasingly problematic for state highway agencies. Regulatory and safety issues have prompted agencies such as the New Mexico State Highway and Transportation Department to look for non-nuclear alternatives for compaction control. This report describes the evaluation of one such commercially available device known as the GeoGauge. The GeoGauge measures soil stiffness, arguably, a much more viable engineering parameter than the moisture-density relations currently used.

The GeoGauge was found to measure soil stiffness as advertised. Results relating moisture, density, and stiffness were found to be consistent with earlier research on compaction and mechanical strength of soils. However, because of the dynamic nature of the measurement obtained via the GeoGauge and associated boundary constraints, the ability to obtain a target value for stiffness in the laboratory has proved to be elusive.

Because of the promising nature of the GeoGauge technology, and because it measures a true engineering mechanical property, a paradigm shift may be necessary for implementation for field compaction control. Future specifications for compaction using this technology may require specific controls of moisture and requirements concerning compaction equipment with stiffness monitoring, via the GeoGauge.

17. Key Words:	18. Distribution Statement
Compaction Control, GeoGauge, Moisture, Density, Soil Stiffness	Available from NMSH&TD Research Bureau

19. Security Classif. (of this report)	20. Security Classif. (of this page)	21. No. of Pages	22. Price
None	None	58	

EVALUATION OF A MECHANICAL STIFFNESS GAUGE FOR COMPACTION CONTROL OF GRANULAR MEDIA

Prepared for:

Research Bureau
New Mexico State Highway & Transportation Department
7500 East Frontage Road
P.O. Box 94690
Albuquerque, NM 87199-4690

Prepared by:

Lary R. Lenke
R. Gordon McKeen
Matt Grush

ATR Institute
University of New Mexico
1001 University Blvd., SE, Suite 103
Albuquerque, NM 87106

December 2001

ACKNOWLEDGEMENTS

Appreciation is extended to ATR Institute research staff who performed the field and laboratory efforts described in this report. Mr. Tom Escobedo, Teaching Laboratory Supervisor, and Mr. Kenny Martinez, Materials Laboratory Supervisor, performed much of the described experimental efforts. Mr. Patrick Reser, undergraduate engineering student, assisted in the experimental work as well. Mr. Kiran Pallachulla, engineering graduate student, is thanked for helping with preparation of portions of the manuscript. Thanks to Ms. Jeanette Albany for her expertise and advice in the use of MS Word and her editorial review. Special thanks are also extended to the ATRI contract and procurement staff who help get the job done, especially Ms. Geri Knoebel and Ms. Debby Pendell.

The research described herein was funded by the Research Bureau, New Mexico State Highway and Transportation Department (NMSHTD). Thanks to Mr. David Albright, Bureau Chief, and Mr. Rais Rizvi, Bureau Research Engineer. Also, thanks to Mr. Stan Mattingly, Research Engineer, and Mr. Steven Von Stein, Pavement Engineer, FHWA, New Mexico Division.

Thanks to Mr. Mel Main, of Humboldt Manufacturing, for suggestions and advice regarding the experimental design and assisting with the data acquired and described in Chapter VI.

TABLE OF CONTENTS

LIST OF FIGURES

LIST OF FIGURES (CONTINUED)

LIST OF TABLES

I. INTRODUCTION

Compaction is the densification of soils by the application of mechanical energy. In general it also involves the modification of the water content. Compaction control of bound and unbound granular soils used in highway construction is necessary to improve their engineering properties. There are several advantages, which occur through compaction, viz.,

1) Detrimental settlements can be reduced or prevented.

2) Soil strength increases and slope stability can be improved.

3) Bearing capacity of pavement subgrades, sub-bases, and base courses can be improved.

4) Undesirable volume changes, for example, caused by frost action, swelling, and shrinkage may be controlled.

Proctor established that compaction is a function of four variables (Holtz and Kovacs, 1981), viz., (1) dry density, (2) water content, (3) compactive effort, and (4) soil type. Consider the common laboratory Proctor test (compaction test) wherein a given soil is compacted into a standard mold with a given compaction energy at varied moisture contents. The classical resultant graph of measured dry density versus moisture content is used to determine the maximum density and optimum moisture content. [1] The maximum density and optimum moisture content are used in specifications for highway construction to ensure proper compaction of respective subgrades, sub-bases, and base courses**.**

While the Proctor test allows the determination of a field target value for compaction control, the actual determination of in-situ density is commonly determined via destructive or

[1] Standard procedures used are described in AASHTO T 99, and T 180, and ASTM D 698, and D1557.

non-destructive field control tests. Destructive tests involve the excavation and removal of some of the intact granular fill material, whereas non-destructive tests determine the density and water content of the granular soil indirectly. Common destructive methods employed are the sand cone method (AASHTO T 191 (ASTM D 1556)), and the balloon density method (AASHTO T 205 (ASTM D 2167)).

Non-destructive determination of density and moisture content using radioactive isotopes has been widely used in lieu of destructive methods for over twenty years now (AASHTO T 238 and T 239 (ASTM D 2922 and D 3017)). Nuclear methods have advantages over the past traditional destructive techniques. Nuclear tests can be conducted rapidly with results known within minutes. Such rapidity allows the contractor and field engineer to know the results quickly, allowing corrective action to be taken as necessary before too much additional earthwork has been placed. More tests per unit time allow a better statistical measure of the compaction control process. Average values of density and moisture content are obtained over a significantly larger volume of fill.

Disadvantages of nuclear methods include their relatively high initial cost and the potential dangers of radioactive exposure to field personnel. Strict radiation safety and training must be enforced with the use of nuclear devices.

The above-mentioned disadvantages of nuclear devices have prompted numerous transportation agencies, including the New Mexico State Highway and Transportation Department (NMSHTD), to look for non-nuclear methods for compaction control. Such alternatives must eliminate the safety and regulatory concerns of nuclear methods, yet it is desirable that any alternatives provide comparable speed and precision during field testing. This desire precludes a step back to the old days of sand cone and balloon density measurements.

Any alternative must also provide a measurand [2] that is related to the engineering properties and engineering performance of the soil evaluated.

The objective of compaction is to stabilize soils and improve their engineering behavior. It is important to keep in mind the desired engineering properties of compacted earthwork, not just its dry density and moisture content. This point is often lost in earthwork construction control. Numerous studies have been performed over the years with regard to engineering properties of soils and the influence of compaction on such properties (Seed and Chan, 1959, Turnbull and McRae, 1950, Turnbull and Foster, 1956). These previous studies focused on mechanical strength properties and how such mechanical properties are affected by compaction. Figure 1 shows the work of Seed and Chan. It clearly shows the effects of compaction energy and moisture content on the strength behavior of a compacted clay material. The strengths of these clay materials tend to decrease, or roll off, as the molding moisture content is increased past the optimum moisture content. Turnbull and Foster also found similar trends. Figure 2 shows a strength parameter (California Bearing Ratio (CBR)) versus compaction energy and moisture content. Again, the CBR decreases as the molding moisture is increased beyond the optimum moisture content for all compaction energies considered.

Typical compaction control specifications require densities that exceed some percentage of the maximum dry density (e.g., 95% of maximum) and moisture contents that are a few moisture content percentage points on either side of the optimum moisture content. Such specifications help to ensure that the mechanical strength (an engineering property) is optimized for a given soil. It is clear that the ubiquitous Proctor curve and field density measurements that

[2] measurand – the physical quantity or property being measured (a technical term not found in your typical English dictionary)

are in use today are, in reality, surrogate measurements that have evolved for ensuring optimal mechanical performance of compacted soils. It is equally clear that such density measurements have been used because of their simplicity and inexpensive nature when compared to more sophisticated strength testing methods.

While strength is known to relate to dry density and moisture content for a given soil, density and moisture content, nonetheless, are not good measures or predictors of engineering properties. It is, however, recognized that material engineering properties such as strength are related to soil stiffness (a mechanical property), which in turn is related to soil modulus (a material property). The latter soil modulus is routinely used in elastic pavement design and influences the pavement structural stiffness and resultant deflections under traffic loadings. Hence, many researchers have focused on the use of simple techniques for measuring the soil modulus or soil stiffness with regard to compaction control. Such stiffness measurements are more fundamentally sound from an engineering perspective than the now universally accepted moisture-density measurements used for compaction control.

The NMSHTD is interested in replacing nuclear devices because of the aforementioned disadvantages of such devices. The ATR Institute at the University of New Mexico was asked by the NMSHTD to identify off the shelf technology that has the potential to replace nuclear devices. The ATR Institute focused on devices that have the ability to provide more meaningful engineering properties, such as soil stiffness or soil modulus, and identified the Humboldt GeoGauge (Stiffness Gauge) as the most promising alternative to nuclear devices. The GeoGauge measures soil stiffness, which can in turn be used to calculate the soil modulus.

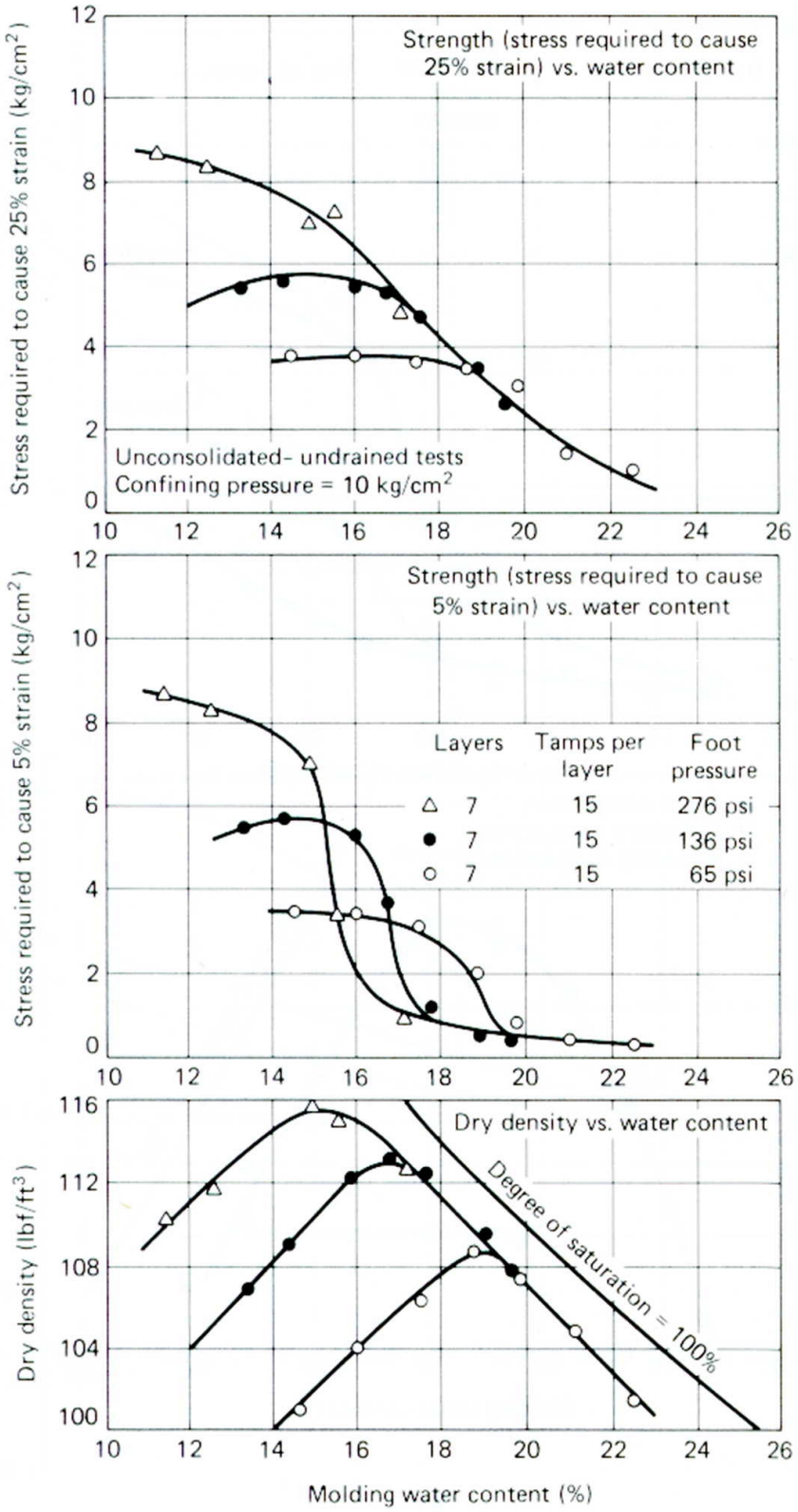

Figure 1. Strength and Density vs. Compactive Energy and Moisture Content (Seed & Chan).

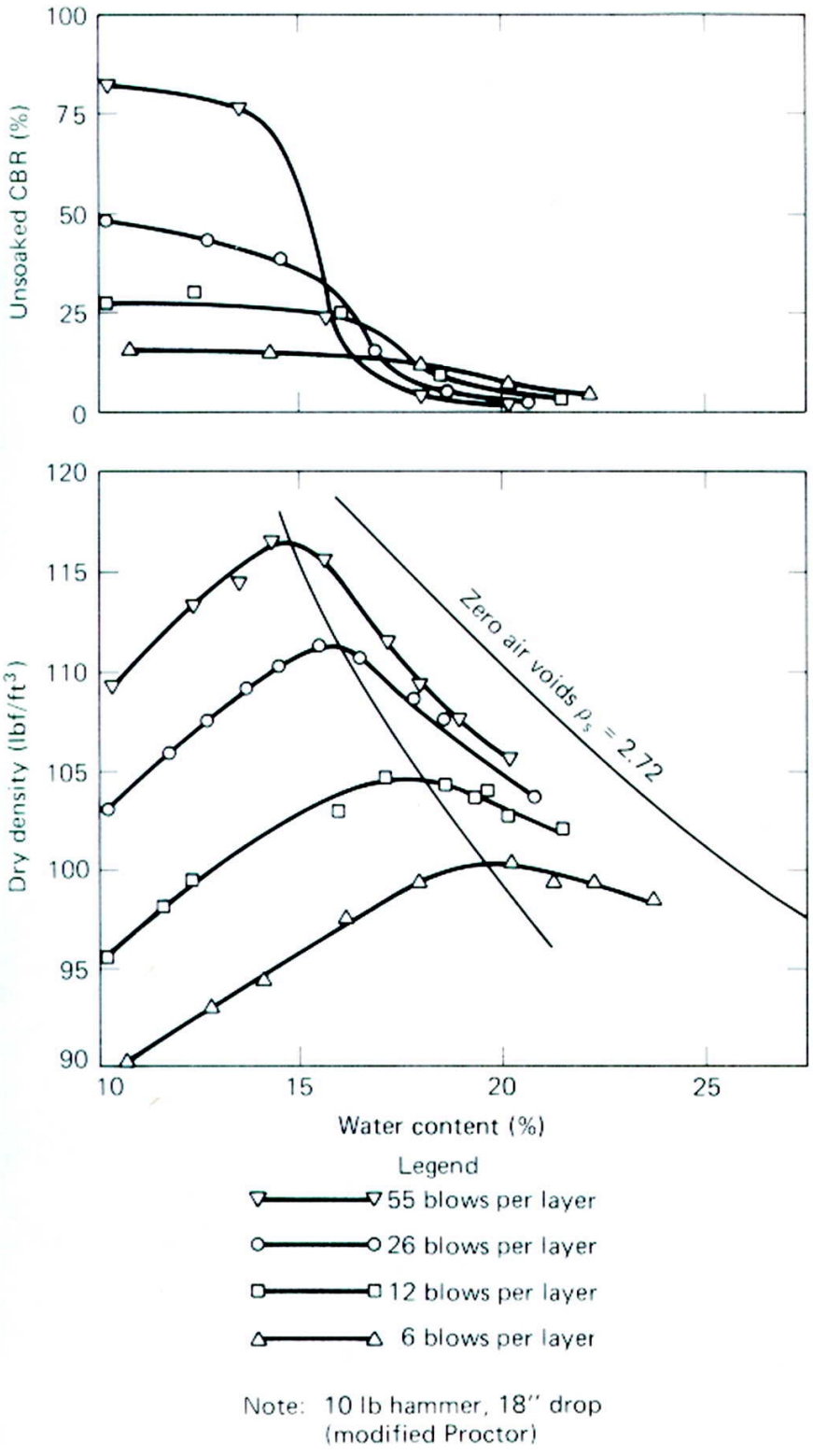

Figure 2. Strength (CBR) and Density vs. Compactive Energy and Moisture Content (Turnbull & Foster).

This report documents an evaluation of the GeoGauge in both laboratory and field environs. Chapter II describes the GeoGauge and its theory of operation. Chapter III presents a laboratory evaluation of the GeoGauge using cohesionless dry silica sand. Chapter IV extends the discussion of Chapter III to a similar evaluation of the GeoGauge on a cohesive soil. Chapter V presents a detailed laboratory experiment that attempts to develop a procedure for ascertaining field target values of stiffness. Chapter VI discusses some experiences with the GeoGauge in actual field operations, including an evaluation of a lime-stabilized material. Chapter VII provides a summary of conclusions and recommendations for further research aimed at eventual implementation of the GeoGauge as a replacement for nuclear devices.

II. GEOGAUGE THEORY OF OPERATION

The GeoGauge, manufactured by the Humboldt Manufacturing Company, is a portable instrument providing a simple and rapid means of measuring the stiffness of compacted subgrade, subbase, and base course layers in earthen construction. The GeoGauge measures stiffness at the soil surface by imparting very small displacements to the soil on an annularly loaded region via a harmonic oscillator operating over a frequency of 100 to 196 Hz. Appropriate transducer technology is incorporated to measure both force and displacement from which stiffness can be computed. The computed stiffness is determined based on an average of 25 stiffness values obtained at 25 discreet frequencies over the frequency band cited above.

The GeoGauge weighs approximately 10 kg (22 lb). The annular ring which contacts the soil has an outside diameter of 4.50 in. (114 mm) and an inside diameter of 3.50 in. (89 mm); hence, with an annular ring thickness of 0.50 in. (13 mm). Humboldt specifications state that the magnitude of the vertical displacement induced at the soil-ring interface is less than 0.00005 in. (1.3×10^{-6} m). The annular foot bears directly on the soil, supporting the weight of the GeoGauge. Attached above this annular footing is a shaker, which excites the footing in a vertical mode. Sensors attached to the shaker and footing are used to measure the force and displacement from which soil stiffness is computed.

Figure 3 presents a schematic of the GeoGauge's cross-section and salient features. The heart of the mechanical system is an electro-mechanical shaker, which drives a flexible plate attached via a rigid cylinder to the rigid annular foot. Matched velocity sensors attached to the flexible plate (V_2) and the rigid annular foot (V_1) allow for the determination of the soil stiffness in the following fashion. The force applied by the shaker (F_{dr}) and transferred to the soil beneath

the rigid foot (F_{soil}) is measured by the differential displacement across the flexible plate as follows:

$$F_{dr} = F_{soil} = K_{flex}(X_2 - X_1) \tag{2-1}$$

where

F_{dr} = the force applied by the electro-mechanical shaker and transferred to the soil

K_{flex} = the flexible plate stiffness

X_2 = the displacement of the flexible plate

X_1 = the displacement of the rigid annular foot.

Differentiation of Equation 1 in the time domain results in the following:

$$\dot{F}_{soil} = K_{flex}(V_2 - V_1) \tag{2-2}$$

where

V_2 = the velocity of the flexible plate

V_1 = the velocity of the rigid annular foot.

Now, the soil stiffness (K_{soil}) is simply

$$K_{soil} = \frac{F_{soil}}{X_1} \tag{2-3}$$

with differentiation yielding

$$K_{soil} = \frac{\dot{F}_{soil}}{V_1} \tag{2-4}$$

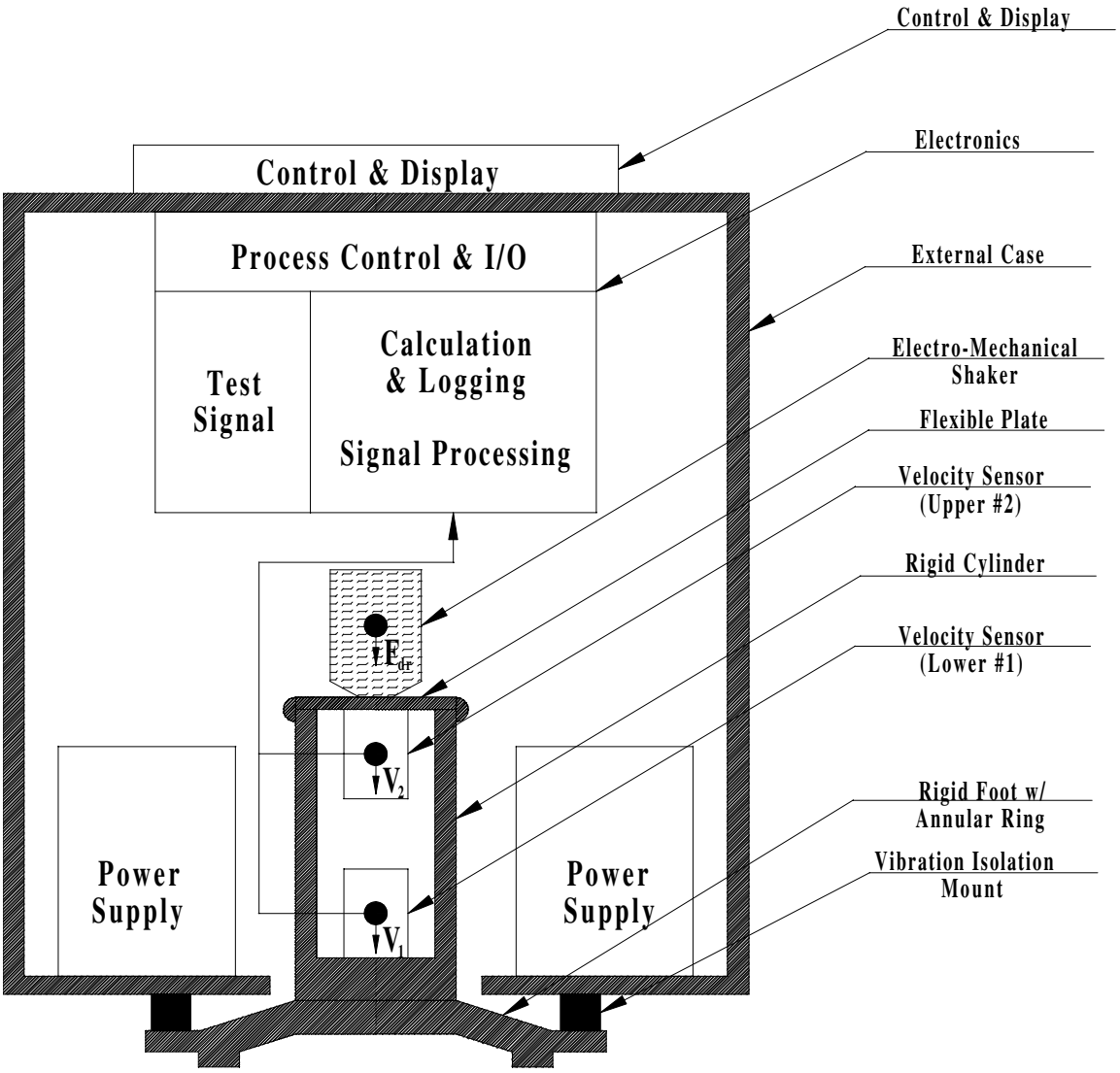

Figure 3. GeoGauge Schematic and Cross-Section (Model H-4140).

Substitution of Equation 2-2 into Equation 2-4 yields an equation for soil stiffness in terms of the measured velocities V_1 and V_2, and the stiffness K_{flex}.[3]

$$K_{soil} = \frac{K_{flex}(V_2 - V_1)}{V_1} \qquad (2\text{-}5)$$

As stated above, the GeoGauge measures the soil stiffness response at 25 discreet frequencies and hence an average value of stiffness is determined ($\overline{K}_{soil}$) via the following formula

$$\overline{K}_{soil} = \frac{K_{flex}}{n} \sum_{1}^{n} \frac{(V_2 - V_1)}{V_1} \tag{2-6}$$

where n equals the number of test frequencies. The above described approach using velocity measurements avoids the need for a non-moving reference for the soil displacement and permits the accurate measurement of small displacements. The GeoGauge was designed assuming the following condition exists, viz., at the frequencies of operation (100-196 Hz), the response is dominated by the stiffness of the underlying soil (the manufacturer specifies a range of stiffness measurement capability from 3 to 70 MN/m).

Figure 3 shows that the velocity transducer signals are processed on an onboard microprocessor with subsequent calculation, logging, and data display. Output is via a user-friendly face panel on the top of the GeoGauge. Power is supplied by six "D" cell batteries.

The measured soil stiffness from the GeoGauge can, in turn, be used to calculate the soil modulus of the underlying bound or unbound soil media. The problem of a rigid annular ring on a linear elastic, homogeneous, and isotropic half space has been considered by Egorov (1965). The static stiffness K of such a soil-structure interaction problem has the functional form

$$K = \frac{ER}{(1-\nu^2)\omega(n)} \tag{2-7}$$

where E and ν are the modulus of elasticity and Poisson's ratio of the elastic media, respectively, R is the outside radius of the annular ring, and $\omega(n)$ is a function of the ratio of the inside

---

[3] K_{flex} is known form established calibration procedures, defined by the manufacturer.

diameter and the outside diameter of the annular ring. For the ring geometry of the GeoGauge, the parameter ω(n) is equal to 0.565, hence,

$$K = \frac{1.77ER}{(1-\nu^2)} \tag{2-8}$$

Now, the modulus of elasticity and the shear modulus (G) are related through $G = \frac{E}{2(1+\nu)}$, hence, the above equation for stiffness can be expressed in terms of shear modulus as

$$K = \frac{3.54GR}{(1-\nu)} \tag{2-9}$$

These equations assume that the underlying soil is linear elastic, homogeneous, and isotropic. They also assume an infinite half space. The assumptions of homogeneity, isotropy, and elasticity are frequently invoked in soil mechanics and pavement design when analyzing soil layers. However, the assumption of an infinite half space is arguably violated when one considers that underlying pavement layers are generally of finite depth (on the order of 6 inches) and are of increasing modulus with depth. Hence, any computation of elastic modulus from the GeoGauge measured stiffness must be carefully evaluated in view of the above assumptions made in the Egorov solution.

This section has briefly described the GeoGauge and its theory of operation. The manufacturer states that the GeoGauge measures stiffness, which can in turn be related to an engineering parameter such as modulus. Such a true engineering parameter is desirable in lieu of surrogate measures such as density and moisture content.

III. EVALUATION ON APPROXIMATE ELASTIC HALF SPACE OF DRY SAND

A first step in evaluation of the GeoGauge is to determine if measured response on known materials is consistent with both theoretical and empirical soil mechanics concepts. It is desirable to evaluate the GeoGauge in a simple laboratory setup and use such theoretical and empirical concepts to verify the stiffness response of the GeoGauge. Such laboratory studies can be problematic except when using the most ideal soils. It has been found that dry uniform sized sands can be used in such studies. However, when performing dynamic soil-structure interaction studies (the GeoGauge and underlying soil are indeed a simple, albeit, small soil-structure problem), one has to be concerned with boundary conditions, wave propagation concerns, and reflected wave energy from near and distant boundaries.

Such dynamic soil-structure interaction experiments were conducted by Lenke, et al (1991), at the University of Colorado, using model footings in an enhanced gravitational field, using the geotechnical centrifuge modeling technique. Because of the inability to truly model an elastic half space experimentally, they evaluated numerous container shapes and boundary materials to minimize reflected wave energy in an attempt to approximate true radiation damping of a vertically excited circular footing. One of the principal conclusions from their research was that cubical containers with a compliant energy absorbing boundary material allowed reasonable approximation of an elastic half space.

Figure 4 (from Lenke, et al) shows the effects of boundary shape and absorbing boundary material on the response of a circular model footing. Figure 4a shows the measured frequency response function for a model footing on the surface of dry sand contained within a cylindrical

aluminum container. [4] Figure 4b shows a similar experiment of the same footing on sand, but with an energy absorbing boundary material on the inside surfaces of the aluminum container. It is clear that the energy absorbing material reduces the energy spikes of the measured frequency response function shown in Figure 4a. The energy absorbing material tends to prevent the magnification or de-magnification (i.e., ringing) of reflected energy from the container boundaries. Figure 3c shows an additional improvement in the response of the model footing by further enhancements of the boundary geometry within the cylindrical container. Finally, Figure 4d shows the effects of using an approximate cubical container lined with the same energy absorbing material. The further improvement is marked, with the frequency response being very close to the theoretical response as described in Lenke et al. The cubical container geometry prevents focusing of transmitted and reflected energy to the source (i.e., the footing), and further helps simulate an elastic half space.

In order to evaluate the GeoGauge, a similar approach was taken, albeit, on a larger scale than the experiments conducted by Lenke, et al. A relatively large steel box was obtained of approximate cubical shape. This steel container is lined with steel plate and reinforced externally by steel channel sections, resulting in a fairly rigid container. The nominal dimensions of this container are 24 in. (610 mm) deep with a lateral cross sectional area of 28 in. by 30 in. (710 mm by 760 mm). The lateral and bottom surfaces of this container were lined with 3/4 in. (19 mm) Styrofoam panels as an energy absorbing material.

[4] A frequency response function (FRF) is a frequency domain representation of the input-output relation for a linear system (see Bendat and Piersol). The data shown in Figure 4 is essentially a frequency domain representation of a force input to a displacement output, i.e., stiffness, of a foundation on an elastic half-space with varied boundary conditions. The GeoGauge also measures stiffness in the frequency domain and averages measured stiffness values over a fairly narrow frequency band.

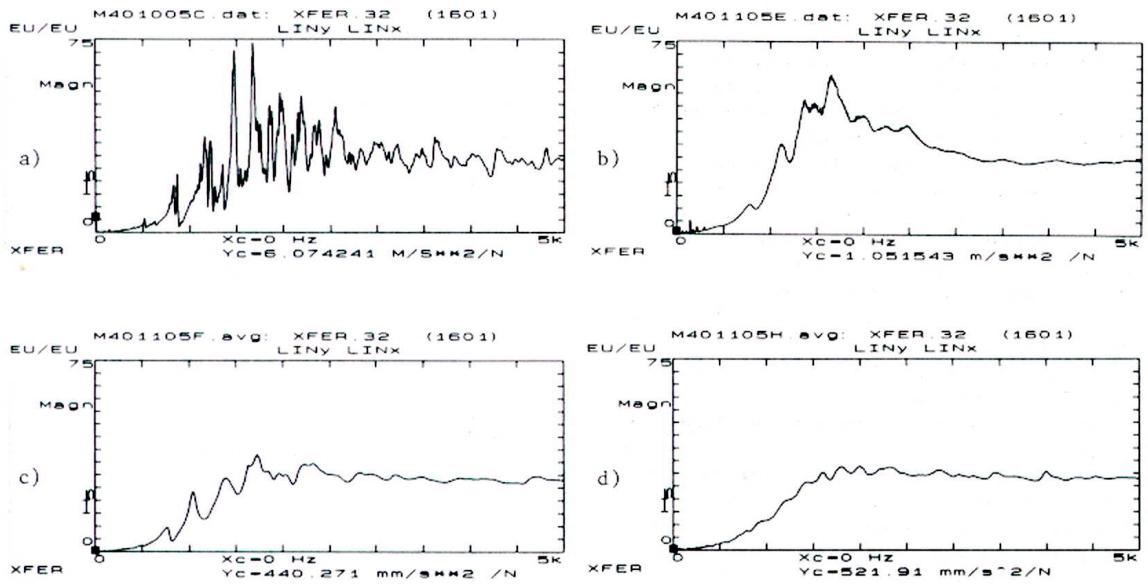

Figure 4. Frequency Response Functions of Model Footings on Dry Sand, a) Cylindrical Container w/o Energy Absorbing Material, b) Cylindrical Container w/ Energy Absorbing Material, c) Cylindrical Container (Modified) w/ Energy Absorbing Material, d) Cubical Container w/ Energy Absorbing Material (Lenke, et al).

A dry granular cohesionless silica sand was obtained from U.S. Silica's Ottawa, Illinois, manufacturing facility. The sand selected was designated as F-52. The product information provided by U.S. Silica states that this sand has a specific gravity of 2.65 (typical of silica sand) with a round grain shape. The mean grain size is approximately 0.26 mm (0.010 in.) based on a tabulated particle size distribution.

This silica sand was then pluviated through air from a height of 18 in. (460 mm) into the foam lined steel test bin described above (see Figure 5). This "raining" operation took approximately 20 hours to accomplish in order to ensure a uniform, highly compact granular media within the test bed. Upon completion of the raining operation, the surface of the sand media was carefully screeded level with the top of the test bin. During this operation the total weight of material placed was carefully tracked. Based on careful measurement of the test bin

dimensions prior to pluviation of the sand, the resultant density of the media within the test bin could be calculated. The average density (unit weight) computed was 110.45 lb/ft^3 (1769.3 kg/ m^3). Based on this unit weight and the known specific gravity, the void ratio of the granular media within the test bin was computed as 0.497 (~100% relative density).

Figure 5. Cubical Test Bin, Sand Raining Operation.

With the granular media now in place within the test bin, measurements of stiffness were obtained using the Humboldt GeoGauge (Figure 6). Measurements were obtained at the center of the test bin surface as well as at quarter points along one diagonal of the square cross section. A total of eight measurements were obtained on centerline with a mean value of 6.19 MN/m (35,300 lb/in.). The standard deviation of these eight measurements was

0.04 MN/m. The associated coefficient of variation, as defined by the ratio of the standard deviation to the mean, was 0.7%.

Figure 6. Cubical Test Bin, Stiffness Evaluation by GeoGauge.

Hardin and Richart (1963) found that the modulus of rigidity (shear modulus) could be related to the void ratio and the mean effective octahedral stress (i.e., average confining pressure) by the following empirical equation.

$$G = \frac{2630(2.17 - e)^2}{(1 + e)} (\overline{\sigma}_o)^{0.5} \qquad (2\text{-}10)$$

where G is the shear modulus, e is the void ratio of the granular media, and $\overline{\sigma}_o$ is the mean confining pressure (bulk stress). The above equation was developed for round-grained sands using dynamic wave propagation experimental methods. The above equation is empirical and has non-homogeneous units. The engineering units of both the shear modulus and mean

effective stress are in terms of pounds per square inch (psi) and apparently the numerical value 2630 has units of $(psi)^{0.5}$.

Equation 2-10 can be used to calculate the stiffness defined previously in Equation 2-9 if the unknown parameters can be estimated with some certainty. The void ratio in Equation 2-10 was very carefully determined during the experimental placement of the sand in the soil test bin. The value of the mean effective stress is much more difficult to ascertain, however. In addition, Poisson's ratio in Equation 2-9 is not known. However, if one can estimate the values of the mean effective stress and Poisson's ratio, then Equations 2-9 and 2-10 can be used to estimate the stiffness of the granular soil in the test bin and a comparison can be made with the GeoGauge experimental value of 6.19 MN/m.

The mean effective stress can be computed using the following definition

$$\bar{\sigma}_o = \frac{\bar{\sigma}_v + 2\bar{\sigma}_h}{3} = \frac{\bar{\sigma}_v + 2K_o\bar{\sigma}_v}{3} = \frac{\bar{\sigma}_v}{3}\left(1 + 2K_o\right) \qquad (2\text{-}11)$$

where $\bar{\sigma}_v$ and $\bar{\sigma}_h$ are the vertical and horizontal effective stress components, respectively, and K_o is the coefficient of lateral earth pressure. The value of K_o can be estimated by an equation developed by Jaky (1944)

$$K_o = \left(1 + \frac{2}{3}\sin\phi\right)\left(\frac{1-\sin\phi}{1+\sin\phi}\right) \qquad (2\text{-}12)$$

where ϕ is the effective angle of internal friction of the granular media. An estimate of this angle of internal friction was obtained by a simple experiment to determine the angle of repose of the F-52 silica sand used in the bin test described previously. The angle of repose measured was 33°. This is considered a lower bound for ϕ; the actual value of ϕ may approach 40° but the lower bound will be used for further computational analysis. Using the angle of repose as an approximation for the internal angle of friction yields a coefficient of lateral earth pressure

of 0.402. Substitution of this value into Equation 2-11 yields the following for the mean effective stress

$$\overline{\sigma}_o = 0.601\ \overline{\sigma}_v \tag{2-13}$$

It can be shown that Poisson's ratio can be estimated using generalized Hooke's law as follows (Wood, 1990)

$$\nu = \frac{K_o}{1 + K_o} \tag{2-14}$$

For the coefficient of lateral earth pressure previously estimated, the value of Poisson's ratio is calculated to be 0.287.

At this point, rational means have been used to estimate all variables for computing the stiffness of the silica sand used in the bin tests with the exception of the vertical effective stress. The value of this vertical effective stress is much more difficult to estimate. The effective stress below the annular footing can be considered as composed of two components. One component is the geostatic, or lithostatic, stress caused by the self-weight of the material. This vertical self-weight component is simply the density (or unit weight) of the material (γ) times the depth below the footing (z). Essentially, the self-weight component of vertical stress is zero at the ground surface of the soil bin and increases in a linear fashion with depth. The second component of vertical stress is caused by the presence of the annular footing on the surface of the experimentally modeled half space.

The analytical solution for the vertical stress distribution on centerline (σ_v) below an annularly loaded footing, at $r = 0$, is presented in Poulos and Davis (1974) as

$$\sigma_v = \frac{3pz^3a}{\left(a^2 + z^2\right)^{5/2}} \tag{2-15}$$

where *a* is the distance from the center of the footing to the centerline of the ring (see Figure 7), *z* is the depth below the centerline of the annular footing, and *p* is an annular line load acting at a distance *a* from the centerline of the footing. For the GeoGauge used in the experiments described previously, *a* is equal to 2.0 in. (51 mm), and the weight of the GeoGauge was measured at 22.01 lb, resulting in an annular line load *p* of 1.752 lb/in. (306.8 N/m).

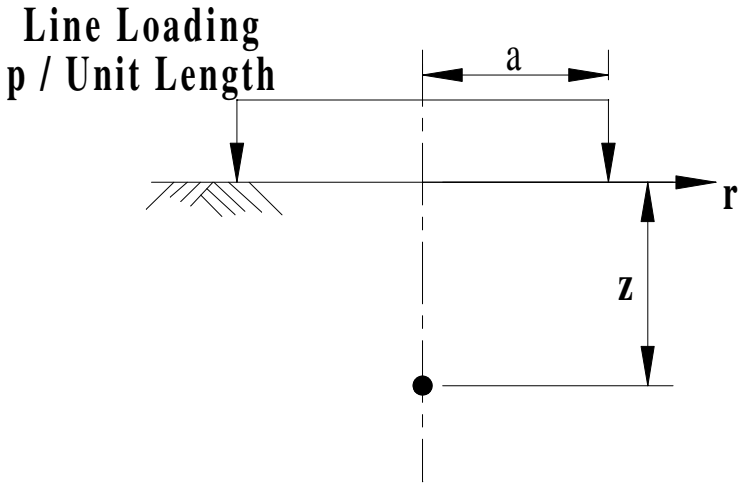

Figure 7. Uniform Vertical Ring Loading on Surface of Elastic Half Space.

Figure 8 shows a graphical representation of the vertical stress distribution as a function of depth for both the geostatic stress component and the annular ring induced component. The sum of these two stress components is the total vertical effective stress. The total stress distribution clearly shows that the stress levels become fairly constant and uniform for depths of 2 to 9 inches (50 mm to 230 mm). It is well known that the "pressure bulb" below a circular footing extends to a depth equal to about twice the diameter of the footing. The dynamic response of the annular footing will also be influenced by a zone of soil to a depth of about two diameters as well. Based on the observed total stress distribution of Figure 8 and a knowledge

that the depth of influence extends to two diameters (9 in.), an estimate of 0.63 psi is made for the vertical effective stress below the annular footing.

Substitution of this estimated 0.63 psi vertical effective stress into Equation 2-13 with subsequent substitution of this bulk stress into Equation 2-10 yields an estimate for the shear modulus of the granular media within the soil test bin. This shear modulus along with the previously estimated value of Poisson's ratio and the outside radius of the GeoGauge annular footing is then substituted into Equation 2-9 yielding a static stiffness of 33,800 lb/in.

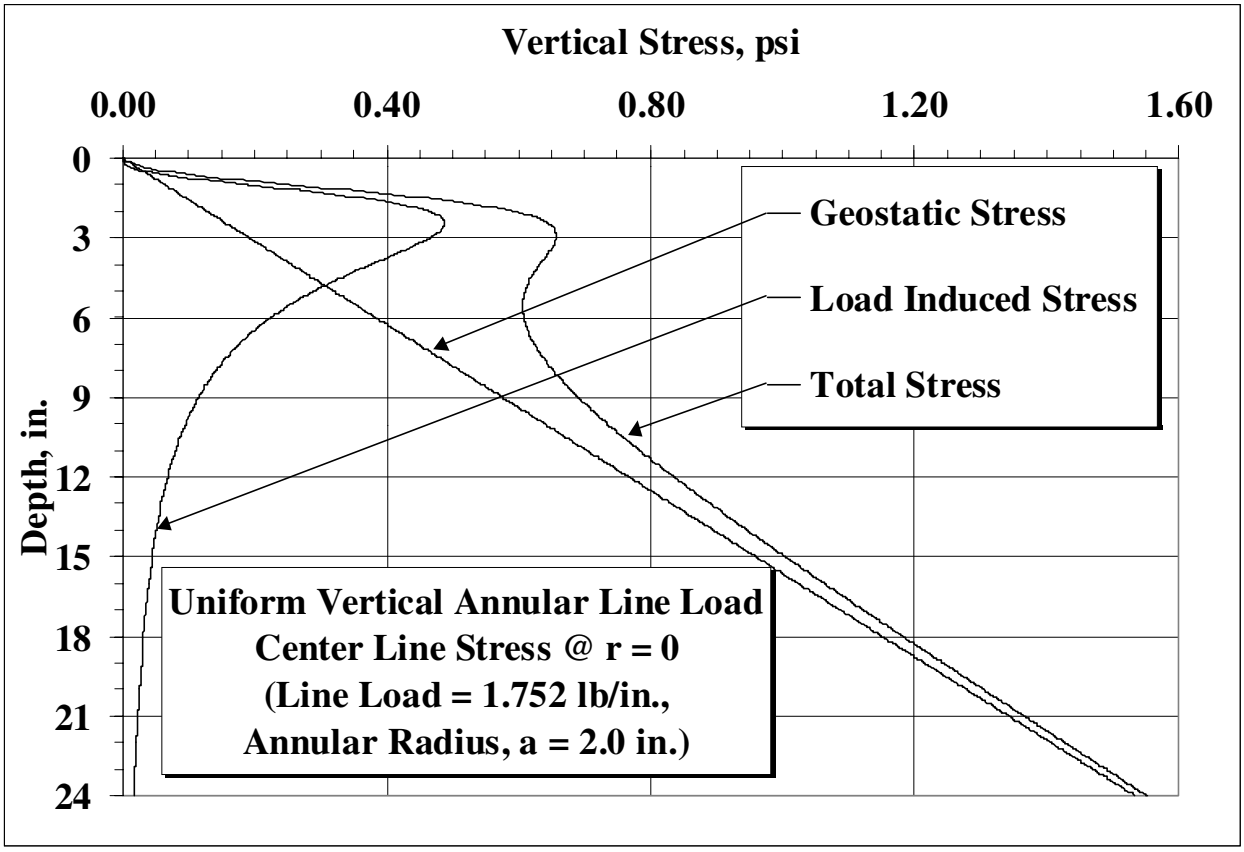

Figure 8. Vertical Stress Distribution Below an Annular Footing.

Comparison of this computational estimate with the experimentally determined value of stiffness (35,300 lb/in) results in an error less than 5%. Based on this simple experiment and a rational soil mechanics analysis, one would conclude that the GeoGauge is indeed measuring the stiffness of the underlying granular soil media.

The effects of layering and proximity to lateral and horizontal boundaries were also investigated using the steel cubical test bin. The same silica sand was rained into place in nominal 4 inch layers using the same raining technique as described above (see Figure 9). Upon completion of placing these 4-inch layers, GeoGauge measurements were made at the center of the test bin (Location 1) and at a location laterally offset from the center towards one corner of the test bin (Location 2).

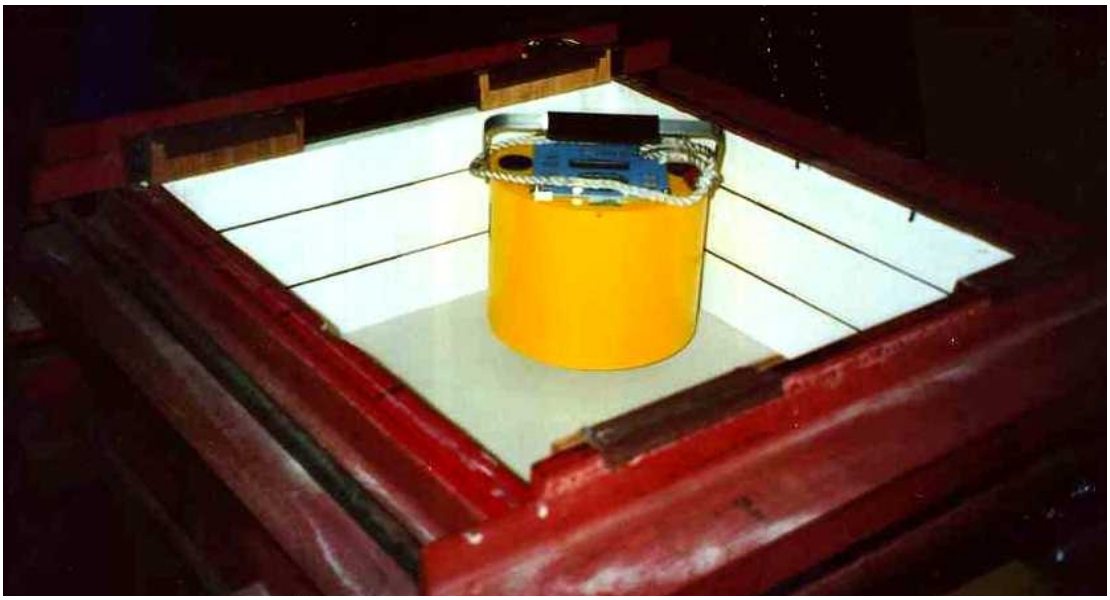

Figure 9. Cubical Test Bin, Layer Stiffness Evaluation by GeoGauge.

Figure 10 presents graphically the results of this progressive measurement of soil stiffness with increasing distance from the bottom horizontal boundary. After placement of the first 4-inch lift, the measured stiffness was approximately 2 MN/m. Subsequent measurements

with increasing depth to the bottom of the soil bin suggest increases in stiffness with a gradual leveling off at a depth of about 12 to 16 inches. At this depth the stiffness stabilizes in the range of 6 to 7 MN/m. It is interesting to note that the measured stiffness at the quarter point toward the corner of the test bin (Location 2) tended to be slightly stiffer that at the measured stiffness at the center of the test bin. This is attributed to the lack of a focusing effect of the reflected energy from the boundaries back to the vibrating source (i.e., the GeoGauge). While the soil bin is cubical in nature and absorbing material is present on the lateral and bottom boundaries, it is doubtful that all reflected energy is completely eliminated. Hence such anomalous differences between locations one and two might be expected.

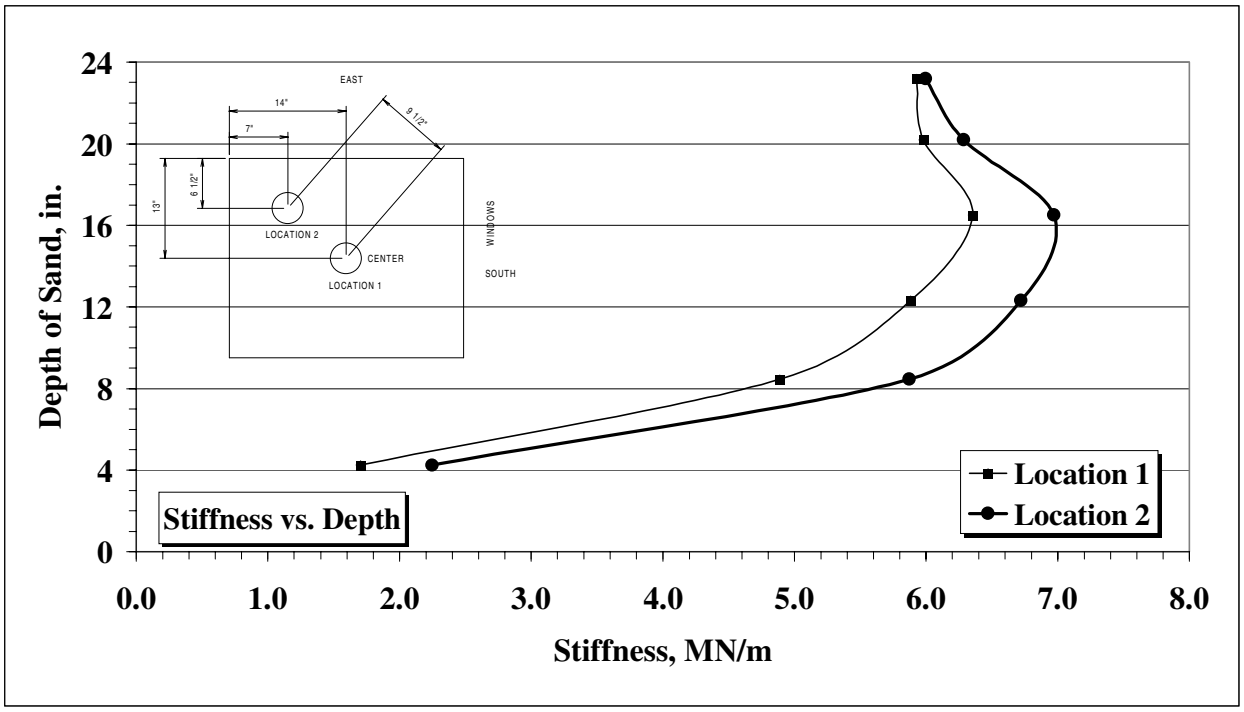

Figure 10. Boundary Effects Evaluation in Cubical Test Bin.

Figure 11 further demonstrates this point. For the last top lift, for a total depth of 24 inches, GeoGauge measurements were made at the 13 locations noted in Figure 11. Stiffness measurements are presented here in terms of the least dimension to a lateral (vertical) boundary.

Locations 1, 5, 6, 9, 10, 11, 12, and 13 are all located at about 5.5 inches from the lateral boundary. Locations 2, 4, 7, and 8 are located at the quarter points towards the corner of the test bin (similar to Location 2 in Figure 10) at about 8 to 10 inches from the lateral boundaries. Location 3 is in the center of the test bin (same as Location 2 in Figure 10) at a distance of 12.5 inches from any lateral boundary. Again it is clear that the GeoGauge response is attenuated for measurements close to the lateral boundary. This is consistent with the observations made previously with respect to the discussion of Figure 10. Stiffness measurements stabilize at a lateral distance from the vertical boundary on the order of 8 to 10 inches.

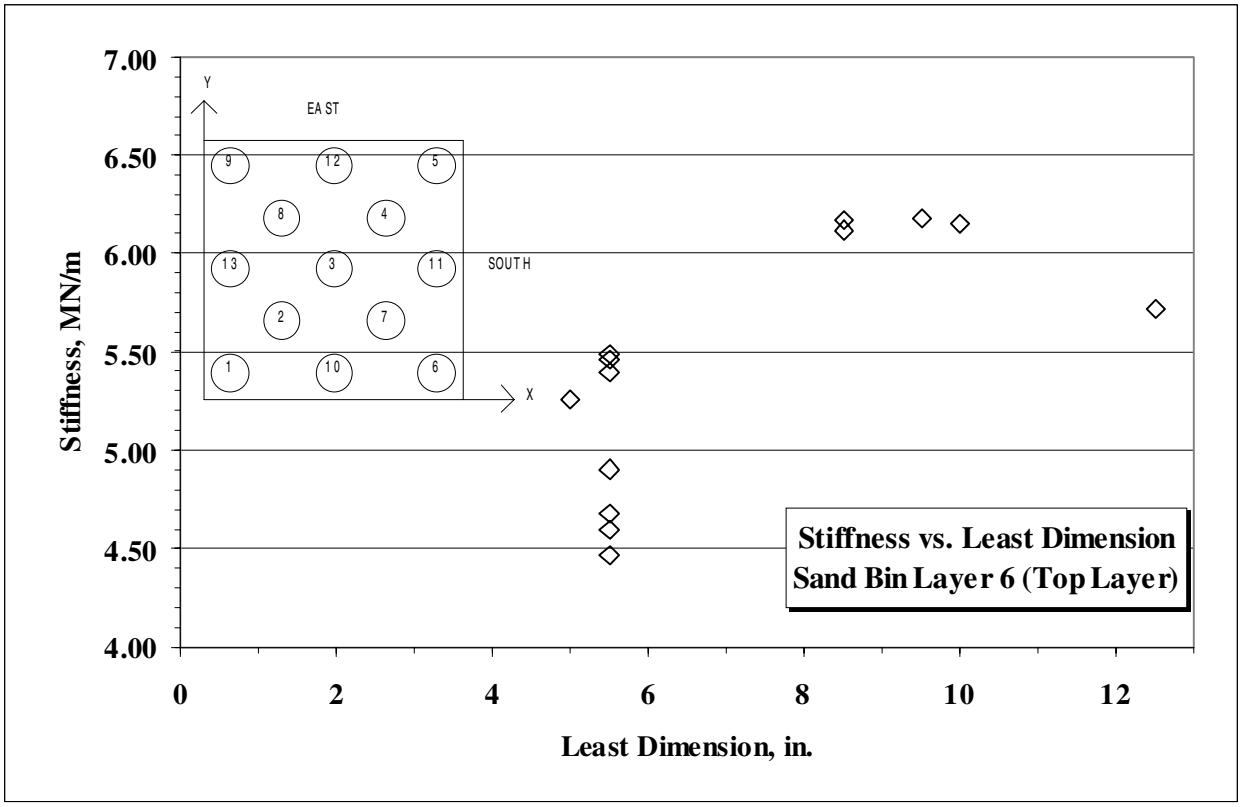

Figure 11. Stiffness vs. Distance to Vertical Boundary.

One can conclude based on these simple experiments that the GeoGauge provides meaningful stiffness results when the distance to horizontal boundaries are on the order of 12 inches deep and the distance to any lateral boundaries is on the order of 9 inches. These numbers are consistent with the GeoGauge manufacturer's claims regarding the minimum layer thickness that may be evaluated and the proximity of buried objects (e.g., metal pipe, concrete structures, etc.).

IV. EVALUATION ON COHESIVE SOIL

One of the principle objectives, in implementing the GeoGauge for field compaction control, is obtaining an objective method for determining an a priori target value for stiffness. Ideally, such a target value should be a laboratory determined value, similar in scope and effort to the methodology used in determining optimum moisture and maximum density. It is clear that the large cubical bin described in the previous chapter is a very time consuming process for the determination of a target value. Furthermore, dry cohesionless sand is never found in the real world of highway construction and compaction control. Subgrades and base course materials are compacted with moisture and tend to have at least some degree of cohesion. These soils lend themselves to densification and increased stiffness by the typical field compaction techniques. Furthermore, laboratory compaction techniques are still a viable method for simulating this field compaction.

The use of the GeoGauge in the laboratory is still problematic because of the boundary effects that have been discussed earlier. In the search for a laboratory standard for stiffness measurement that can be translated to the field, some compromises are inevitable in order to achieve a test method that is relatively quick to perform, yet provides some definition of stiffness potential for a given soil. The evaluation of a more typical cohesive soil requires the use of a scaled down version of the sand bin of the previous chapter. It is also desirable to ascertain the relation between density, stiffness, and moisture content in a more reasonably sized soil container.

Thus, the first step in attempting to define a laboratory target value for stiffness using cohesive soil was to use a smaller soil test container. A double plied reinforced plywood box, with a wall and base thickness of 1.5 inch, was constructed with nominal dimensions of 15 inch

by 15 inch cross-section by 12 inch depth; a volume of 1.56 ft^3. Plywood was selected for this soil bin because of its superior energy absorbing properties compared to steel. Figure 12 shows this soil container partially filled with compacted soil.

A cohesive silty-sand, an AASHTO A-2-4 material (Unified classification: SM), was compacted into this soil bin using a standard Proctor compaction energy. A standard 10 pound Marshall hammer, used for asphalt compaction, was modified with a 4 inch by 4 inch steel plate attached to its base. Six lifts were compacted into the container to full depth. To achieve the standard Proctor energy, the 10-pound hammer was dropped through its 18-inch drop height 228 times per lift. The last lift was trimmed flush with the top of the soil container for subsequent testing by the GeoGauge. This described process was replicated for six different moisture contents.

Figure 13 shows the actual testing with the GeoGauge on the surface of the cohesive soil. After evaluation with the GeoGauge, the plywood sides were removed, and the sample was split in half for moisture content evaluation (see Figure 14). Approximately 2 kg of soil was removed from the internal section of these two halves along the entire depth of the sample for subsequent drying and moisture content calculation.

The volume of soil for this test was markedly reduced compared to the sand bin tests previously described, yet the effort to obtain one stiffness measurement with corresponding density and moisture content was considerable. To obtain one set of measurements with associated sample preparation, container assembly and disassembly takes in excess of 4 hours. To obtain a complete set of stiffness and density parameters, for various moisture contents, takes the better part of three man days.

Figure 12. Plywood Soil Bin for Cohesive Soil (note compaction hammer).

Figure 13. GeoGauge Testing on Plywood Soil Bin with Cohesive Soil.

Figure 14. Moisture Content Evaluation (Full Depth).

Figure 15 presents the results from evaluation of this cohesive silty-sand. The upper graph shows the dry density versus moisture content. The maximum dry density is noted to be 116 lb/ft^3 and the optimum moisture content is 12 %. In contrast to the density plot, the lower graph shows that the maximum stiffness, as measured with the GeoGauge, is at a lower moisture content. The maximum stiffness of 25 MN/m occurs at moisture content of about 7 %. This "phase" shift is not surprising in view of the discussion presented in Chapter 1. Seed and Chan's work and that of Turnbull and Foster both suggest that peak mechanical response of a soil material may peak before the point of optimum moisture content as defined in terms of dry density. Their data clearly shows a "roll off" in mechanical response as the moisture content is increased beyond the point of the peak mechanical response. The lower graph clearly shows this "roll off" as the stiffness approaches zero at a moisture content of about 13 %.

The results of Figure 15 must be viewed with some judgment since the effects of the lateral boundaries and focusing effects are not known. It is clear that this relatively small container does not simulate the ideal elastic half space. However, the results are consistent with previous studies cited in Chapter 1. The lower graph of Figure 15 suggests a "roll off" to zero stiffness, which was observably not true, as the soil was still able to support its own weight upon removal of the plywood forms (similar to the view of Figure 14). It is possible for the GeoGauge to respond with a zero output, or even a negative stiffness value (which is physically impossible, as stiffness by definition must be positive). Recall Equation 2-5 for the calculation of stiffness. If the value of velocity transducer #1 is equal to or less than the value of velocity transducer #2, then the GeoGauge measured (computed) stiffness will be zero or non-positive. Clearly when this occurs, the GeoGauge is operating on a soil for which it was not designed or on a geometry with boundary conditions for which it was not designed or intended, as well.

The other clear and obvious conclusion is that the development of a target value using the described plywood soil bin is extremely time consuming for one soil let alone the numerous soils expected on a typical construction project. Any laboratory procedure defined for obtaining a stiffness target value must be accomplished in a time frame consistent with that necessary to obtain the common Proctor density curve.

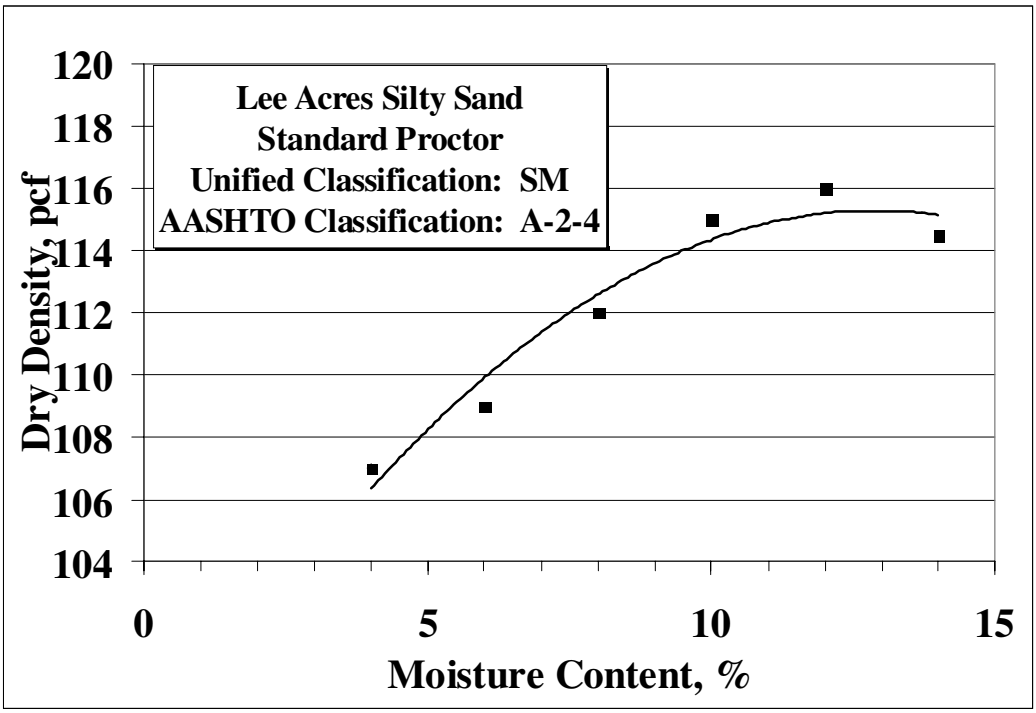

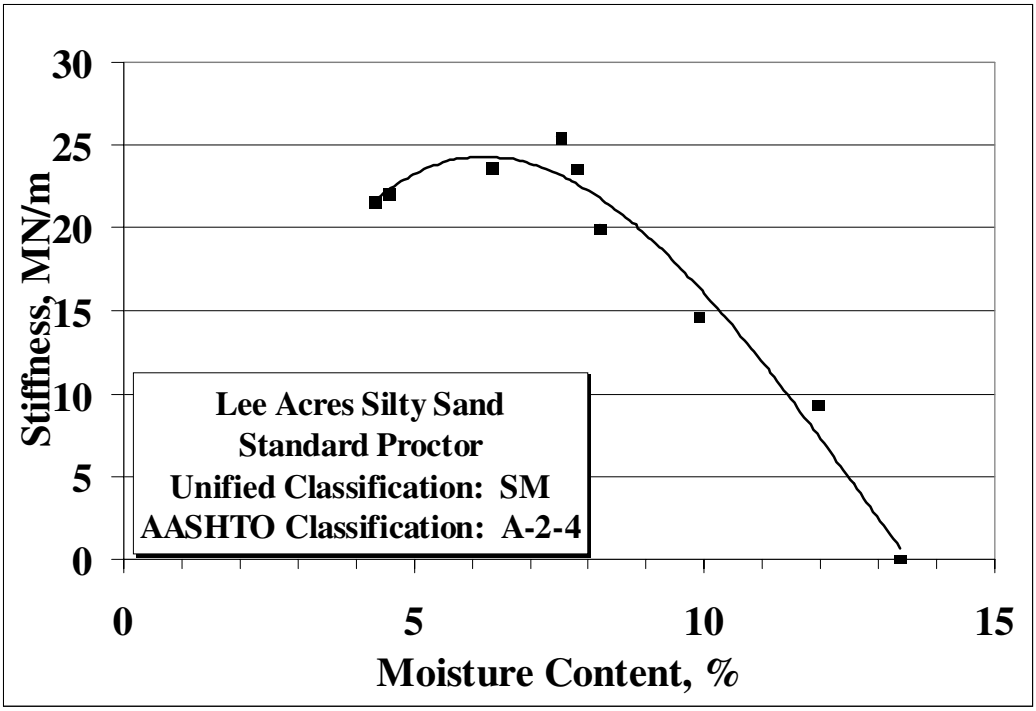

Figure 15. Density and GeoGauge Stiffness vs. Moisture Content for Cohesive Soil.

V. STIFFNESS TARGET VALUE USING CYLINDRICAL PROCTOR MOLDS

In view of the considerable time necessary to obtain a target value with the aforementioned plywood soil bin, it was decided to attempt obtaining target values using cylindrical proctor molds. Modified molds were chosen because of their larger internal diameter of 6 inches in contrast with the more common standard proctor mold of 4-inch diameter. It should be stated at the outset that this decision to obtain a target value with small molds is fraught with concerns. It has been argued previously in this report that boundary concerns are very real when making dynamic measurements. The closer the boundaries are to the excitation source presents concerns about the value of the GeoGauge measurand and whether it is indeed measuring the soil stiffness or some dynamic combination of the soil and proctor mold. Nonetheless, such an experiment was undertaken because of the efficiency with which such samples could be made and evaluated.

The GeoGauge measures stiffness in a 3-dimensional fashion based on the way wave energy radiates from the vibrating source (foot). It was felt that an additional independent dynamic measurement might be useful to corroborate or substantiate the GeoGauge measurements. A one-dimensional wave propagation technique, commonly used for evaluating portland cement concrete (ASTM C 597), was selected because of its simplicity. This experimental technique, known as Pulse Velocity (PV) because of it one-dimensional measurement, is minimally sensitive to the proctor mold constraining the soil material. As such, the PV test can be used to ascertain the soil modulus as well as a stiffness that can be compared to the GeoGauge measurement. The standard PV test used for concrete testing uses a pair of 54 kHz transducers. For the testing of soil in proctor molds, a pair of 24 kHz transducers was

also used to evaluate the subsequently described soils. The 24 kHz transducers are more suitable for the lower modulus of soil and the finer particle sizes of soil in contrast to those of concrete.

The experiment is quite simple. Three soils were evaluated. Each soil was compacted into modified steel proctor molds at varied moisture contents. In addition, to quantify the effects of compaction energy, three different compaction energies were used on each soil as well. One set of GeoGauge measurements were determined by placing the proctor mold with soil on a concrete pedestal (see Figure 16). A second set of GeoGauge measurements were obtained by placing the mold with soil on a concrete floor (see Figure 17). In addition to GeoGauge stiffness and PV measurements using 24 and 54 kHz transducers, density and moisture were carefully measured as well. Lastly, because of concerns about the appropriateness of steel molds, the same experiment was also conducted on molds made of acrylic. Table 1 shows the complete test matrix employed.

Figure 18 is a schematic showing the two GeoGauge test configurations. The first configuration is the evaluation of stiffness in a Proctor mold attached to a concrete pedestal. Note the presence of the customary base plate attached to the concrete pedestal and the wing nuts used to clamp a retainer plate at the top of the proctor mold (these are clearly visible in Figure 16). The second configuration where the soil in the proctor mold is placed on the concrete floor shows that any clamping or restraint of the mold was not employed.

Three soils were evaluated during this experiment. Soil #1 is a free-draining sandy material used for mechanically stabilized earth wall construction. It is classified as an AASHTO A-1-b(0). Soils #2 and #3 are silty-sandy materials used for compacted subgrade, classified as A-2-4(0) and A-2-4 materials, respectively. All three soils were obtained during construction activity from the reconstruction of the I-25 and I-40 interchange in Albuquerque, New Mexico.

Figure 16. GeoGauge Test on Soil on Concrete Pedestal (note acrylic mold).

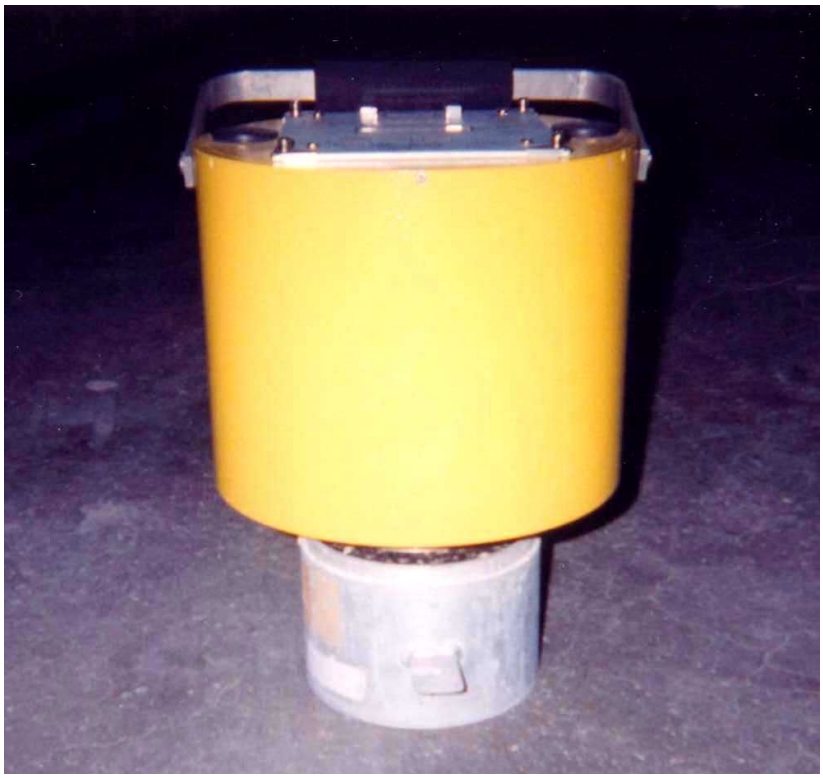

Figure 17. GeoGauge Test on Soil on Concrete Floor (note steel mold).

Table 1. Test Matrix for Target Value Determination Using Modified Proctor Molds

		Steel Mold				Acrylic Mold			
	Compactive Energy	GeoGauge (Pedestal)	GeoGauge (Floor)	Pulse Velocity (54 kHz)	Pulse Velocity (24 kHz)	GeoGauge (Pedestal)	GeoGauge (Floor)	Pulse Velocity (54 kHz)	Pulse Velocity (24 kHz)
Soil 1 (A-1-b(0))	45 % Std. Proctor	$w_1, w_2, w_3, \ldots$	$w_1, w_2, w_3, \ldots$	$w_1, w_2, w_3, \ldots$	$w_1, w_2, w_3, \ldots$	$w_1, w_2, w_3, \ldots$	$w_1, w_2, w_3, \ldots$	$w_1, w_2, w_3, \ldots$	$w_1, w_2, w_3, \ldots$
	Std. Proctor	$w_1, w_2, w_3, \ldots$	$w_1, w_2, w_3, \ldots$	$w_1, w_2, w_3, \ldots$	$w_1, w_2, w_3, \ldots$	$w_1, w_2, w_3, \ldots$	$w_1, w_2, w_3, \ldots$	$w_1, w_2, w_3, \ldots$	$w_1, w_2, w_3, \ldots$
	Mod. Proctor	$w_1, w_2, w_3, \ldots$	$w_1, w_2, w_3, \ldots$	$w_1, w_2, w_3, \ldots$	$w_1, w_2, w_3, \ldots$	$w_1, w_2, w_3, \ldots$	$w_1, w_2, w_3, \ldots$	$w_1, w_2, w_3, \ldots$	$w_1, w_2, w_3, \ldots$
Soil 2 (A-2-4(0))	45 % Std. Proctor	$w_1, w_2, w_3, \ldots$	$w_1, w_2, w_3, \ldots$	$w_1, w_2, w_3, \ldots$	$w_1, w_2, w_3, \ldots$	$w_1, w_2, w_3, \ldots$	$w_1, w_2, w_3, \ldots$	$w_1, w_2, w_3, \ldots$	$w_1, w_2, w_3, \ldots$
	Std. Proctor	$w_1, w_2, w_3, \ldots$	$w_1, w_2, w_3, \ldots$	$w_1, w_2, w_3, \ldots$	$w_1, w_2, w_3, \ldots$	$w_1, w_2, w_3, \ldots$	$w_1, w_2, w_3, \ldots$	$w_1, w_2, w_3, \ldots$	$w_1, w_2, w_3, \ldots$
	Mod. Proctor	$w_1, w_2, w_3, \ldots$	$w_1, w_2, w_3, \ldots$	$w_1, w_2, w_3, \ldots$	$w_1, w_2, w_3, \ldots$	$w_1, w_2, w_3, \ldots$	$w_1, w_2, w_3, \ldots$	$w_1, w_2, w_3, \ldots$	$w_1, w_2, w_3, \ldots$
Soil 3 (A-2-4)	45 % Std. Proctor	$w_1, w_2, w_3, \ldots$	$w_1, w_2, w_3, \ldots$	$w_1, w_2, w_3, \ldots$	$w_1, w_2, w_3, \ldots$	$w_1, w_2, w_3, \ldots$	$w_1, w_2, w_3, \ldots$	$w_1, w_2, w_3, \ldots$	$w_1, w_2, w_3, \ldots$
	Std. Proctor	$w_1, w_2, w_3, \ldots$	$w_1, w_2, w_3, \ldots$	$w_1, w_2, w_3, \ldots$	$w_1, w_2, w_3, \ldots$	$w_1, w_2, w_3, \ldots$	$w_1, w_2, w_3, \ldots$	$w_1, w_2, w_3, \ldots$	$w_1, w_2, w_3, \ldots$
	Mod. Proctor	$w_1, w_2, w_3, \ldots$	$w_1, w_2, w_3, \ldots$	$w_1, w_2, w_3, \ldots$	$w_1, w_2, w_3, \ldots$	$w_1, w_2, w_3, \ldots$	$w_1, w_2, w_3, \ldots$	$w_1, w_2, w_3, \ldots$	$w_1, w_2, w_3, \ldots$

a) $w_1, w_2, w_3, \ldots$ are moisture contents to generate the density and stiffness curves vs. moisture contents (note that these moisture contents will vary from cell to cell within the matrix)
b) 45% of Standard Proctor Energy = 5,500 ft•lb/ft^3
Standard Proctor Energy = 12,400 ft•lb/ft^3
Modified Proctor Energy = 56,000 ft•lb/ft^3
c) Soils are classified per AASHTO

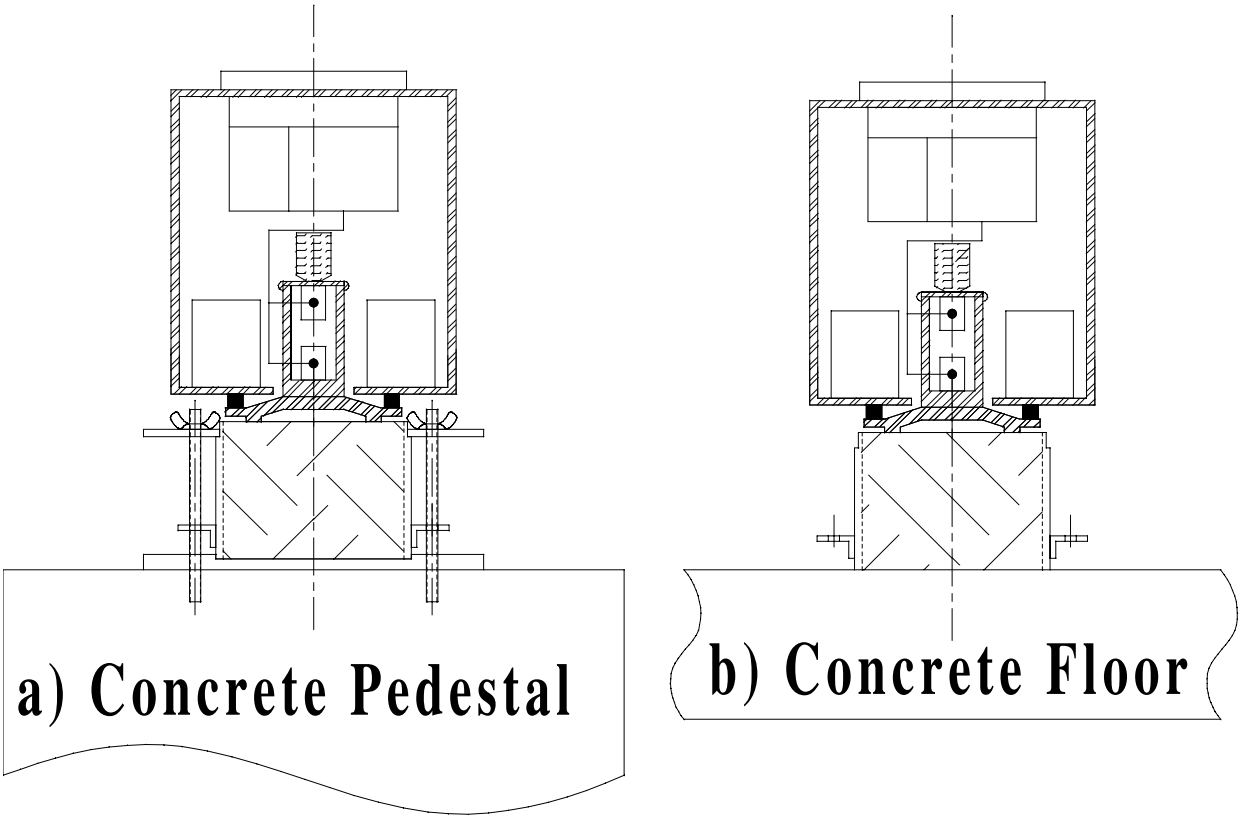

Figure 18. GeoGauge Test Schematic for Tests on Soil in Modified Proctor Molds, a) Test on Concrete Pedestal, b) Test on Concrete Floor.

The different soils were compacted into 6-inch diameter modified proctor molds made of steel or plastic at varied moisture contents. The essence of AASHTO test method T 180 was followed during the varied compaction processes. The standard Proctor effort of 12,400 ft•lb/ft^3 was achieved by placing 3 lifts and compacting each lift 56 times with a 5.5 lb hammer dropped from a 12 inch height. The 45 % of standard Proctor effort of 5,500 ft•lb/ft^3 was obtained by placing 3 lifts and compacting each lift 25 times with a 5.5 lb hammer dropped from a 12-inch height. The modified Proctor effort of 56,000 ft•lb/ft^3 (~450 % of standard Proctor effort) was achieved by placing 5 lifts and compacting each lift 56 times with a 10 lb hammer dropped from a height of 18 inches. After compacting each sample, GeoGauge and PV measurements were made along with density and moisture content determinations.

The pulse velocity measurements were obtained on the soil within the proctor molds as depicted in Figure 19. The bottom transducer is placed on a set of slotted plates for egress of the instrumentation cable. The soil sample within the Proctor mold is then centered on top of this bottom transducer. The top transducer is then placed on top of the soil specimen. To ensure a consistent contact pressure between the transducers and the soil specimen, a 2 kg slotted plate is placed on top of the top transducer. The PV device measures the transit time of one-dimensional pulses from one transducer to the other transducer. When the distance between the transducers is known (the sample length in this case), the velocity of the pulse can be computed as follows

$$V_d = L/t \tag{5-1}$$

where

V_d = the dilatational wave speed of the soil

L = the soil specimen length (4.58 in)

t = the measured transit time of the one-dimensional pulse.

Because of the lateral constraint of the Proctor mold, the computed pulse velocity is considered to be dilatational velocity as opposed to a rod velocity (an unconstrained velocity).

The above determined dilatational velocity can be used to compute what is known as a constrained modulus (related for isotropic materials to the Young's modulus or shear modulus) as follows

$$C = \rho V_d^2 \tag{5-2}$$

where

C = the constrained modulus

ρ = the mass density of the soil specimen (note: this is not the unit weight or dry density, but the mass per unit volume).

The dilatational velocity can also be used to compute the Young's modulus of elasticity (E) for an assumed value of Poisson's ratio (ν) via the following equation

$$E = \frac{\rho V_d^2 (1+\nu)(1-2\nu)}{(1-\nu)} \tag{5-3}$$

For computations where this Young's modulus of elasticity is determined based on pulse velocity measurements, Poisson's ratio is assumed equal to 0.35.

The constrained modulus can be converted to a soil stiffness value by the following equation

$$K = \frac{CA}{L} \tag{5-4}$$

where A equals the cross-sectional area of the soil specimen. Presenting the pulse velocity measurements in terms of soil stiffness allows for a more ready comparison with the soil stiffness values obtained with the GeoGauge.

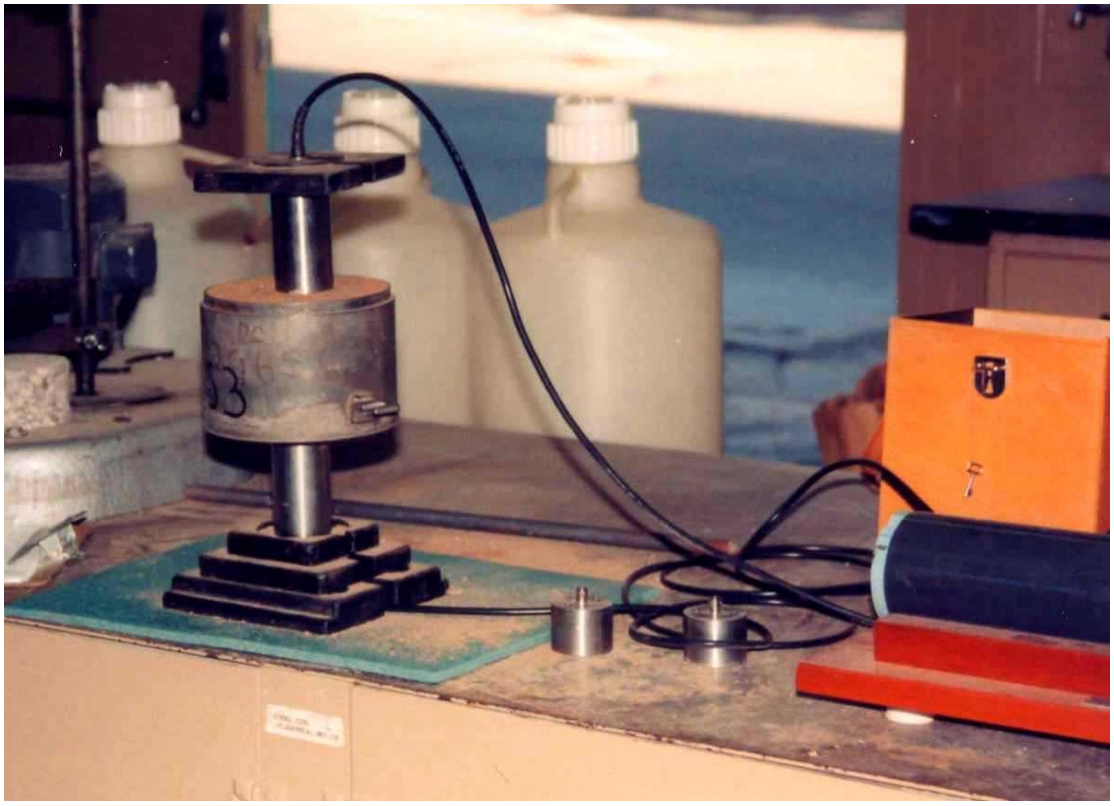

Figure 19. Pulse Velocity Measurements on Soil Within Proctor Mold.

It is worthwhile to compare the difference between GeoGauge measurements made on the concrete floor versus those made on the concrete pedestal. Figure 20 presents graphs for both the steel mold and acrylic mold tests for all three soils compacted and tested at a standard Proctor energy. These graphs suggest that there is little difference between modulus determinations made on the two different concrete surfaces. The pedestal appears to be about 10% stiffer based on linear regression, but the scatter is sufficiently high to make this slight difference insignificant. Comparison of these two graphs also suggests that there is little difference between the measurements made in steel versus acrylic molds; most of the measurements for both steel and acrylic were between 0.04 and 0.10 GPa. The modulus values

shown in this figure were computed using Equation 2-8 for an assumed value of Poisson's ratio of 0.35. Graphs for the other two compaction energies produce similar results and conclusions.

A similar comparison of pulse velocity measurements using 24 and 54 kHz transducers is shown in Figure 21. One can conclude from these graphs that there is little difference, for practical purposes, between the 24 and 54 kHz transducers for the soils evaluated. Again the magnitudes of Young's modulus between the steel and acrylic molds appear to be insignificant.

Both the GeoGauge measured stiffness and computed PV stiffness are mechanical properties. As such, it is expected that these stiffness values will vary with moisture content and compactive effort in a fashion similar to those discussed in Chapter 1 (Seed & Chan and Turnbull & Foster). It was shown earlier that there is no practical significant difference between GeoGauge measurements on a concrete floor compared to a concrete pedestal, or significant differences between pulse velocity transducers (24 kHz vs. 54 kHz), or significant differences between steel and acrylic Proctor molds. Therefore, the discussion to follow will be limited to GeoGauge test results obtained on the concrete pedestal, pulse velocity measurements obtained using the 54 kHz transducer pairs, and compaction performed in the steel Proctor molds.

Figure 22 shows the moisture-density relations obtained for the three soils using the three different compaction energies. Note that the different compaction energies result in clearly distinguishable loci. This is true for each of the three soils, as would be expected, and is consistent with the classical references cited previously in Chapter 1. Also note that the data for Soil #1 is not as spread out with respect to density (sensitive to compactive effort) as for the other two soils. This is expected for a sandy soil in contrast to the cohesive Soils #2 and #3.

One would also expect that a mechanical property plotted versus moisture content would result in very distinguishable loci for different compaction energies. Figure 23 shows plots of

pulse velocity stiffness versus the moisture content for the three soils evaluated. This figure clearly shows that the mechanical property being measured by the pulse velocity technique is sensitive to compaction energy. The only soil for which this is problematic is for Soil #1 which, being a sandy material, is not very sensitive to density changes with different compaction energy, and hence not very sensitive to stiffness change with different compaction energy. Figure 23 clearly shows that as the compaction energy is increased there is a corresponding increase in stiffness at a given moisture content. Again, this is quite consistent with the work cited earlier (Seed and Chan, Turnbull and Foster).

Figure 24 shows measured GeoGauge stiffness versus moisture content for the three soils evaluated at three different compaction energies, in similar fashion to Figure 23. One would expect that the loci of points representing different compaction energies would be quite distinct and separate. This is not the case. For some moisture contents, the stiffness measurements of the soil compacted with modified effort are less than that for the same soil compacted with the sub-standard, 45 %, effort. There is no clear trend, for any of the three soils evaluated, of increasing stiffness with increasing compaction energy as would be expected. Viewing the three graphs suggest that the peak stiffness measurements for all three soils are essentially the same; in the range of 8 to 12 MN/m. It's not clear that the stiffness measurements are those of the soil or of some combined effect of the soil, proctor mold, and bottom boundary configuration. It is clear, though, that the GeoGauge as used in this configuration is unable to discriminate an increase in stiffness with an increase in compaction energy. One can only conclude that trying to obtain a stiffness target value on a volume of soil comparable in size to the foot of the GeoGauge is not possible.

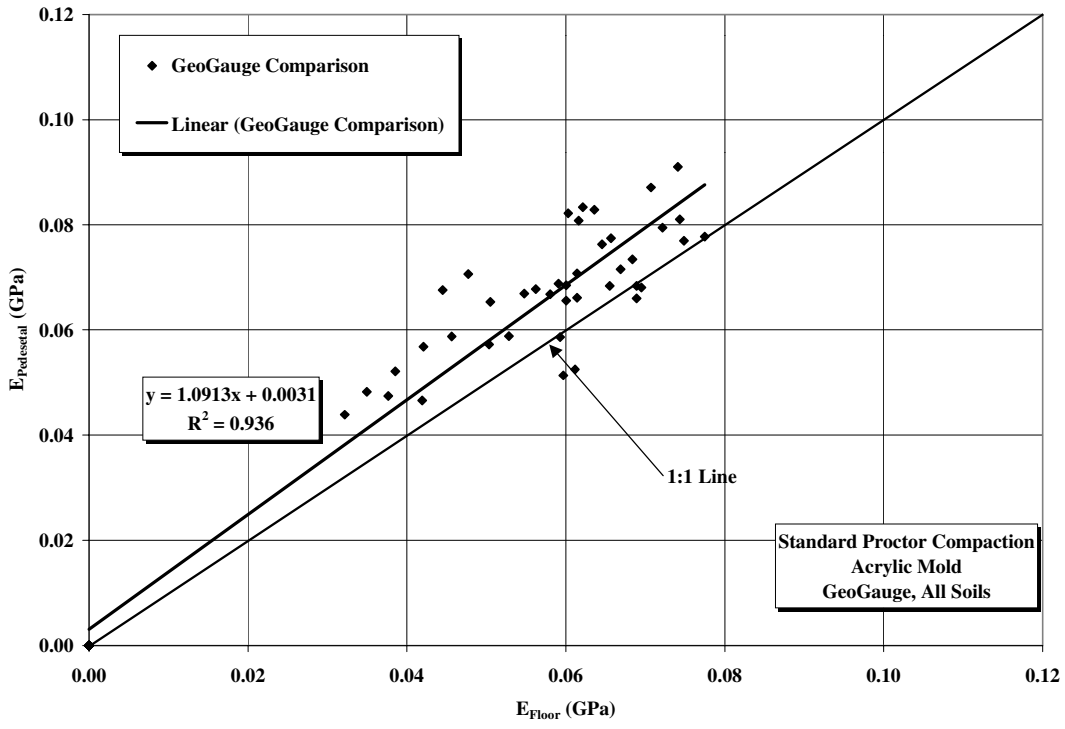

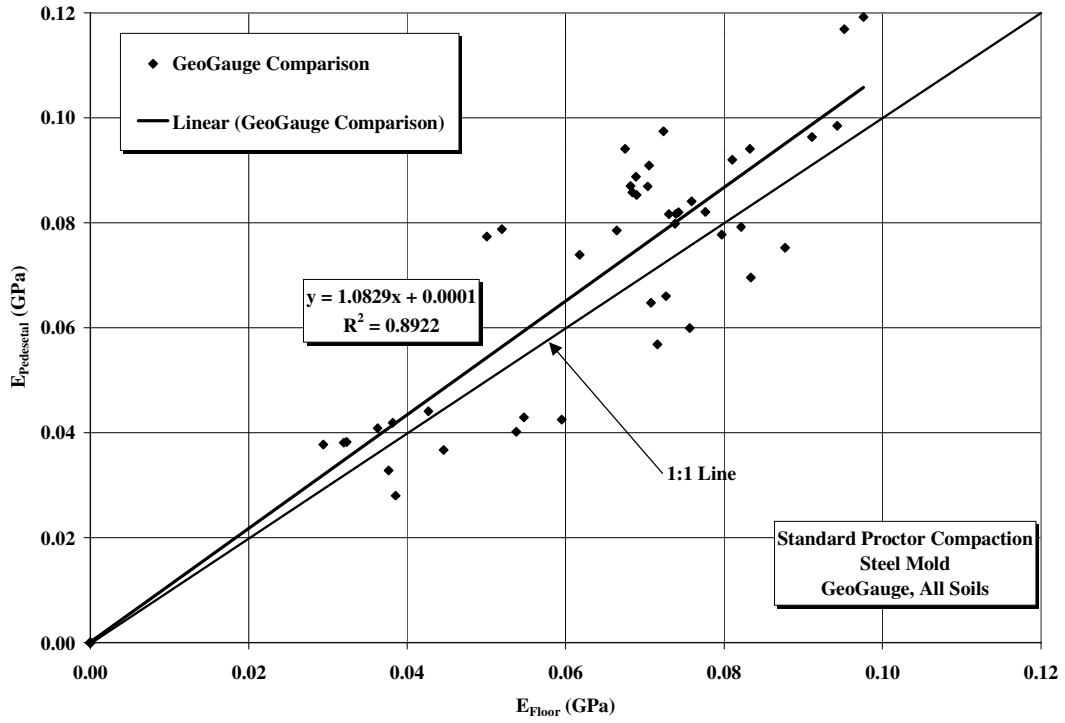

Figure 20. Comparison of GeoGauge Measurement on Pedestal vs. Floor.

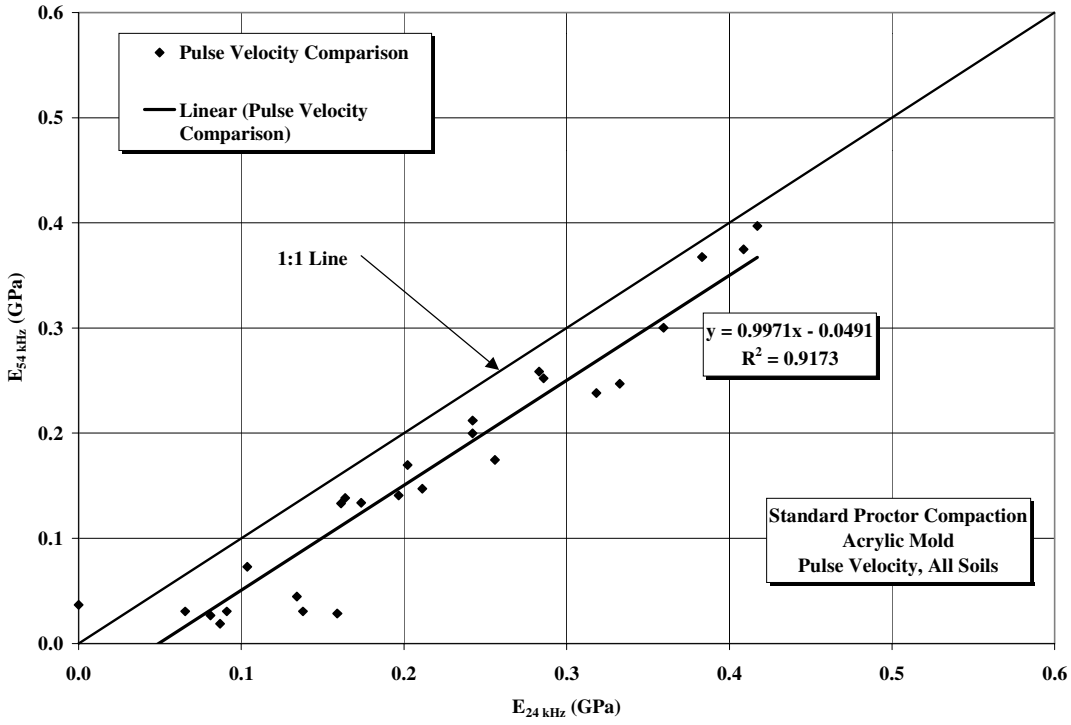

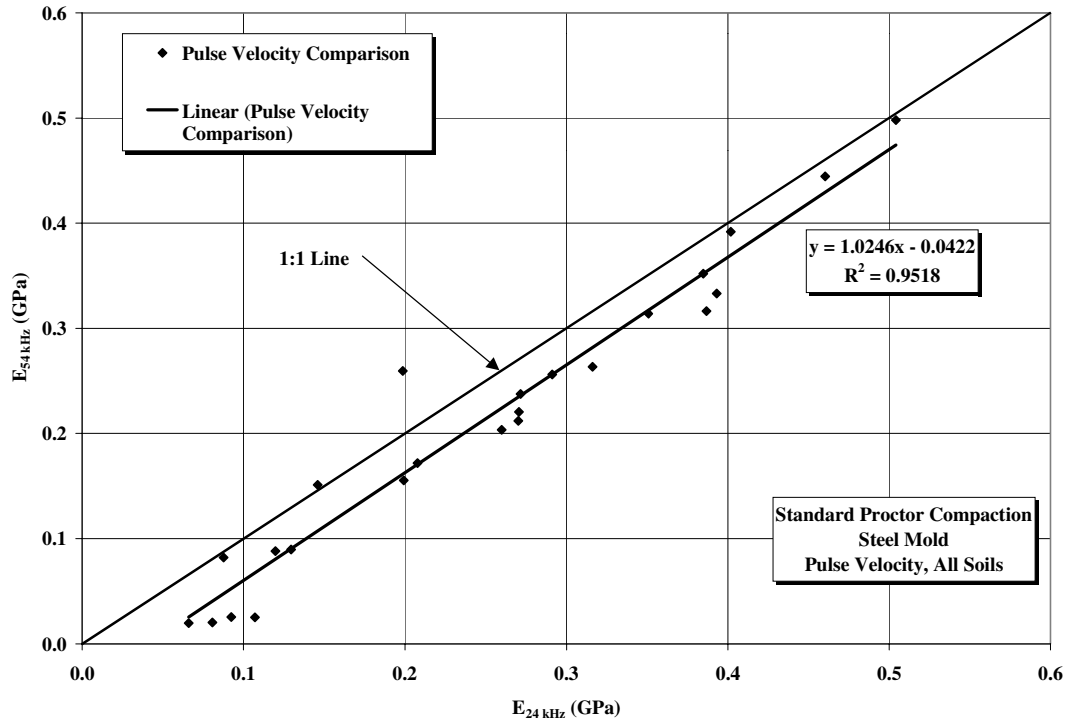

Figure 21. Comparison of Pulse Velocity Measurements (54 vs. 24 kHz).

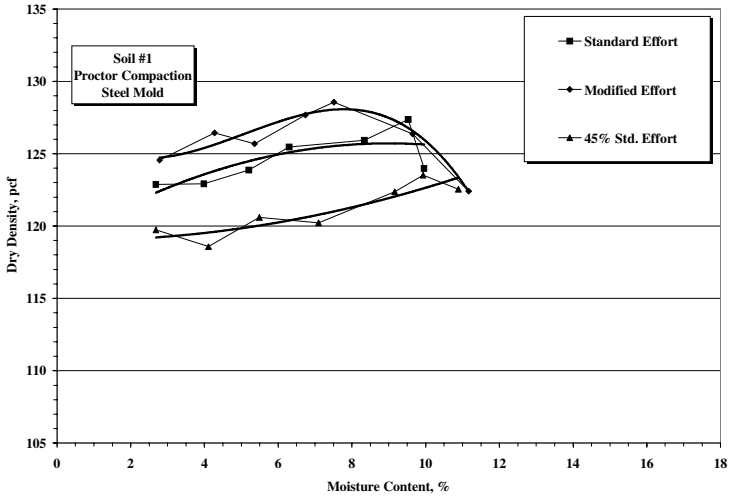

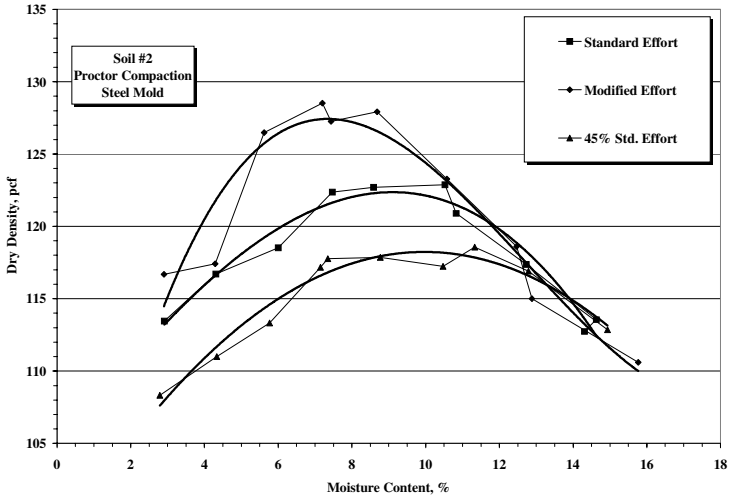

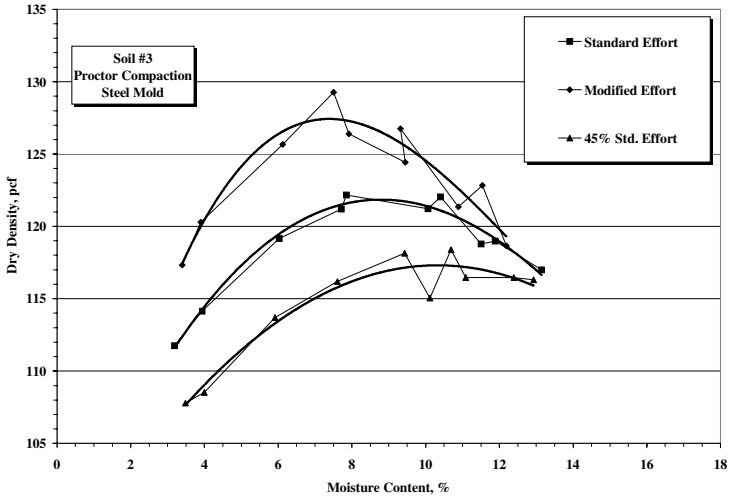

Figure 22. Moisture Density Relations for All Soils.

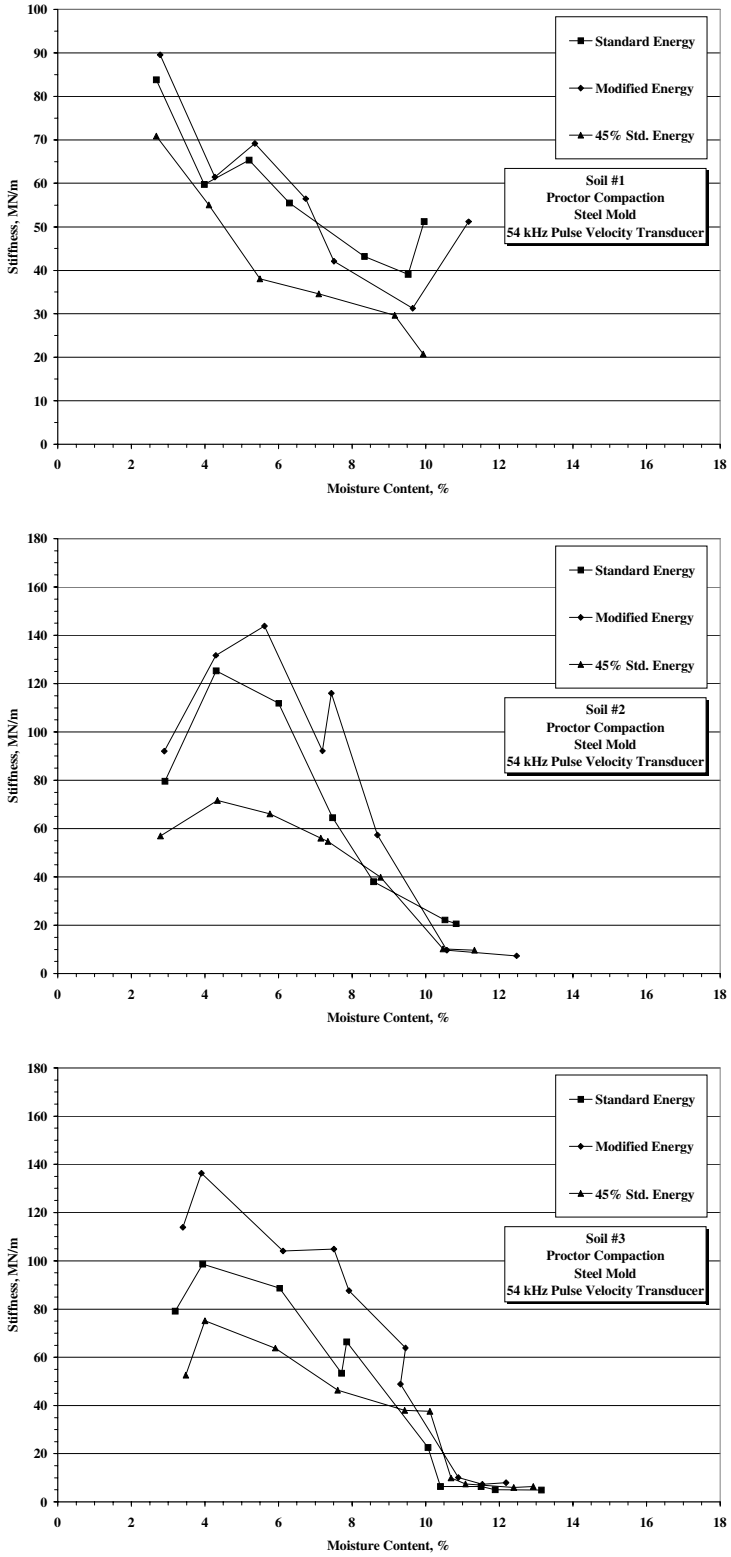

Figure 23. Pulse Velocity Stiffness vs. Moisture Content for All Soils.

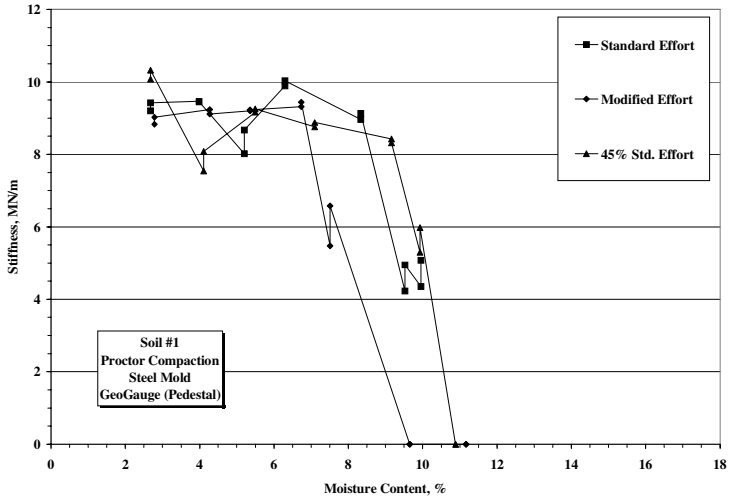

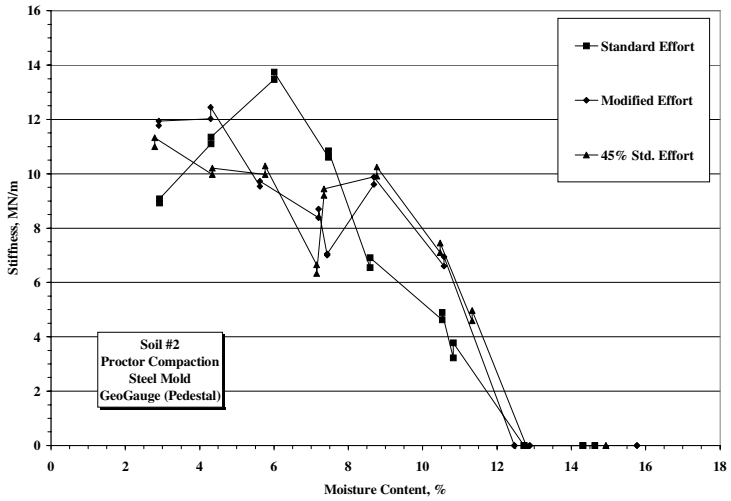

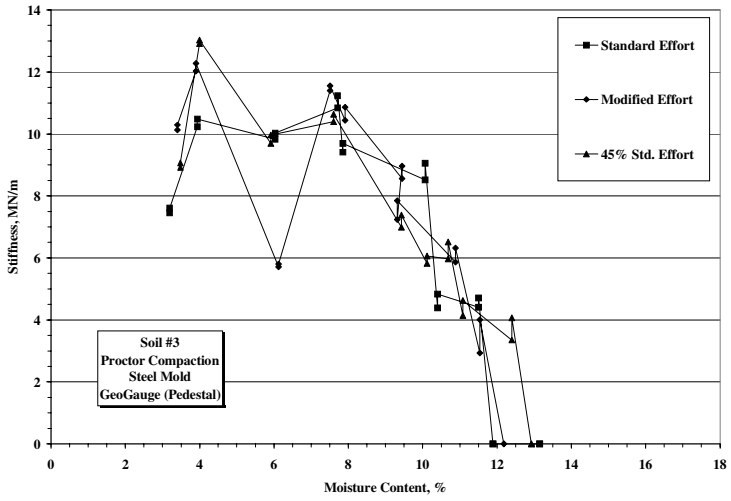

Figure 24. GeoGauge Stiffness vs. Moisture Content for All Soils.

The main concern for obtaining a target value for a dynamic stiffness measurement, such as the GeoGauge, is one of boundary conditions and focusing of reflected wave energy from these boundaries back to the source (i.e., the vibrating annular foot). The wave energy bouncing around in the small volume of the Proctor mold is quite complex, and surely chaotic in nature. Wave energy is reflected and refracted off of the lateral boundaries as well as off the horizontal bottom and top boundaries (the top boundary being the annular footing). In addition, the soil is surely not uniform throughout the soil volume and layering effects due to the compaction process make uniformity even more questionable. Density within layers is not constant and even the thickness of individual specimens can vary and surely will vary between different specimens. Symmetry of the GeoGauge on the surface of the Proctor specimen will also produce non-symmetric and chaotic wave reflections. The ratio of the diameter of the foot of the GeoGauge to the diameter of the Proctor mold is 0.75. The aforementioned experiments of Lenke, et al made use of model footings less than 10% the size of the soil container, and reflected wave energy was of considerable concern without the use of energy absorbing material on the container boundaries.

The above considerations, all verbiage, are perhaps illustrated best with a simple illustrative example. Figure 25 shows an analogous geometry demonstrating the complex nature of wave propagation in a very finite volume (Kolsky, 1953). This figure shows the propagation of wave energy from a point source on the edge of a Perspex (acrylic) plate, a very uniform and homogeneous material. This point source is a small charge of lead azide explosive at the center of the upper edge (analogous to the annular line load of the GeoGauge). The right edge of each photo within Figure 25 is analogous to the centerline (line of symmetry) of the GeoGauge. The

Perspex plate represents the underlying soil. It is also worthwhile to note that acrylic has mechanical elastic properties, both modulus and Poisson's ratio, similar to that of soil.

At 10.5 μs and at 21.7 μs the expanding wave front is radially symmetric and well behaved. At 34.3 μs the wave front impinges on the left boundary (equivalent to the Proctor mold boundary) and right boundaries (centerline of the GeoGauge) and both compressional and shear wave energy is reflected off of these boundaries. At 60.8 μs the wave front hits the bottom boundary (equivalent to the bottom of the Proctor mold) and is reflected as well. By 93.5 μs the nature of the wave energy is obviously quite complicated, and this is only *one* cycle of excitation. The GeoGauge is exciting such an upper boundary as the Perspex plate 100 to 200 times per second. Clearly the wave fronts propagating from such a source are interacting in a very complex and chaotic fashion. Hence, it is not surprising that the response of the GeoGauge on soil with similar boundary conditions is not well behaved and provides stiffness values that are not consistent with known theory as the compaction energy is varied.

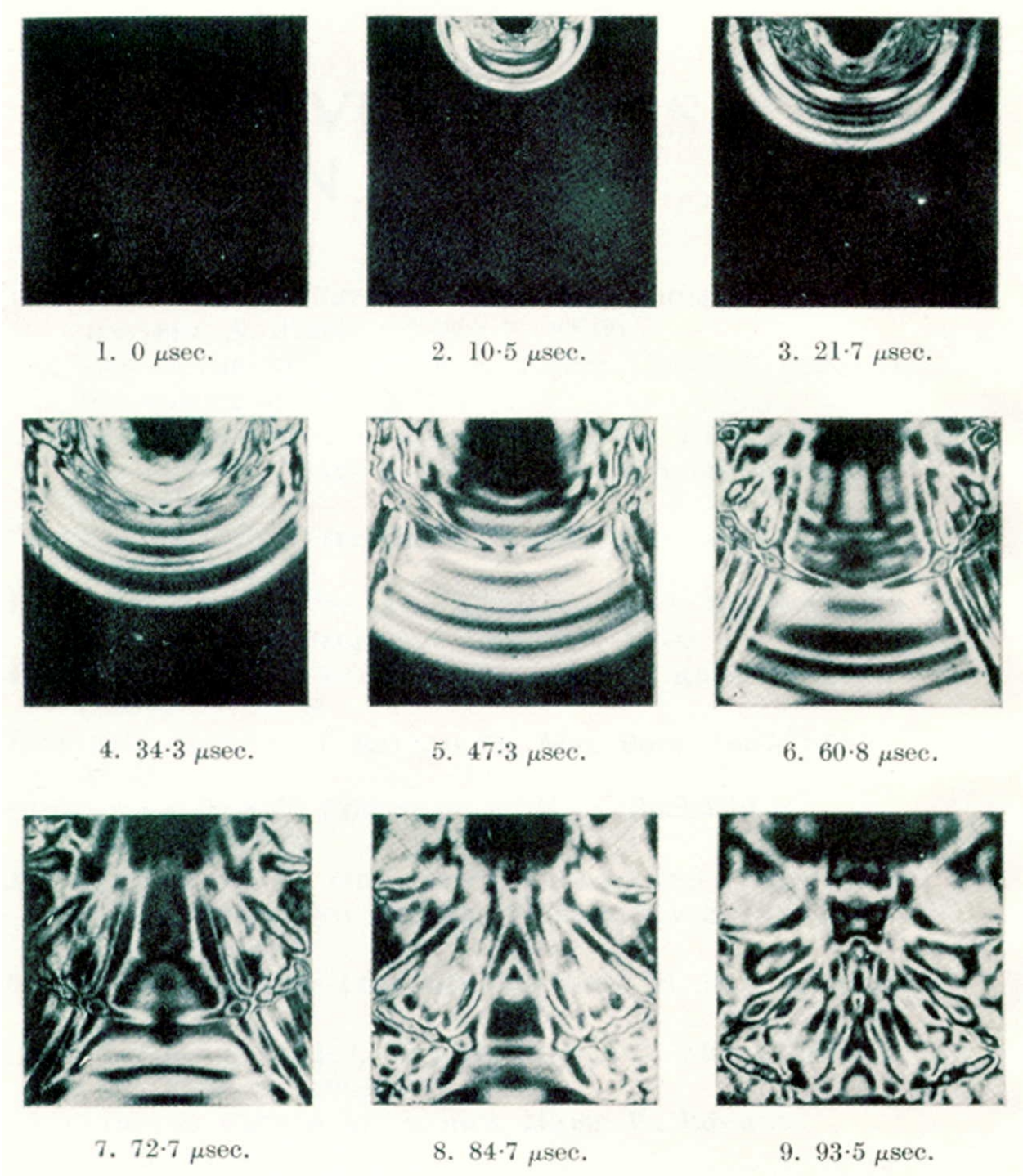

Figure 25. Stress Waves Produced in a 5.5 by 5.5 by 0.25 inch "Perspex" Plate by a Charge of Lead Azide Explosive Detonated at the Center of the Upper Edge (times given are measured from the instant of detonation), 1) 0 μs, 2) 10.5 μs, 3) 21.7 μs, 4) 34.3 μs, 5) 47.3 μs, 6) 60.8 μs, 7) 72.7 μs, 8) 84.7 μs, 9) 98.5 μs (Kolsky).

VI. FIELD STIFFNESS TESTING

The major thrust of this report has focused on laboratory evaluation. A limited amount of field experimentation was conducted. In view of the fact that the GeoGauge cannot discriminate between compaction energies when tested on a small volume of soil within a Proctor mold, it was felt necessary to verify if the GeoGauge can discriminate stiffness increases in the field as compaction progresses.

The GeoGauge was used to evaluate stiffness increase as a function of roller passes on a base course material on an approach ramp on the Big-I (I-25 & I-40) reconstruction. The approach ramp evaluated was the west bound to north bound ramp. Six locations on this ramp were monitored via GeoGauge stiffness measurements as compaction occurred. Figure 26 shows a plot of measured stiffness versus the number of roller passes. The roller was a steel wheeled vibratory roller. Figure 26 clearly shows that the stiffness increased with the number of roller passes. In contrast to the laboratory, the GeoGauge can indeed discriminate increases in stiffness with increased compactive effort during field use.

An additional field data set was obtained on the reconstruction of New Mexico State Highway 44 (now designated as U.S. 550). Lime stabilization was used extensively during this reconstruction project to stabilize subgrade materials. Four distinct locations (stations), with similar soil, were identified for GeoGauge stiffness evaluation. One location was used as a control with no lime stabilization, the other three locations had been stabilized with lime and had cured in-situ for different periods of time; the first for one day, the second for 2 days, and the third for two weeks (14 days). Twenty-one (21) stiffness measurements were made at each station on an equally spaced 20 by 30 foot grid. Figure 27 is a photograph showing these field GeoGauge measurements as well as companion dry-density measurements using a nuclear

density device. Table 2 shows the results of this study. Note that the mean stiffness increases with curing age for these lime stabilized materials. The variation of GeoGauge measurements across the test grid is quite reasonable as indicated by the fairly low coefficient of variations. Also note that the dry density at each location is the same regardless of curing age indicating that stiffness is a good indicator of strength gain of these stabilized materials, while density clearly is not. Figure 28 presents graphically the results of this table. Again it is clear that stiffness, and therefore strength, increases with time during this curing process of lime stabilized materials. Such use of the GeoGauge in these applications appears to be compelling.

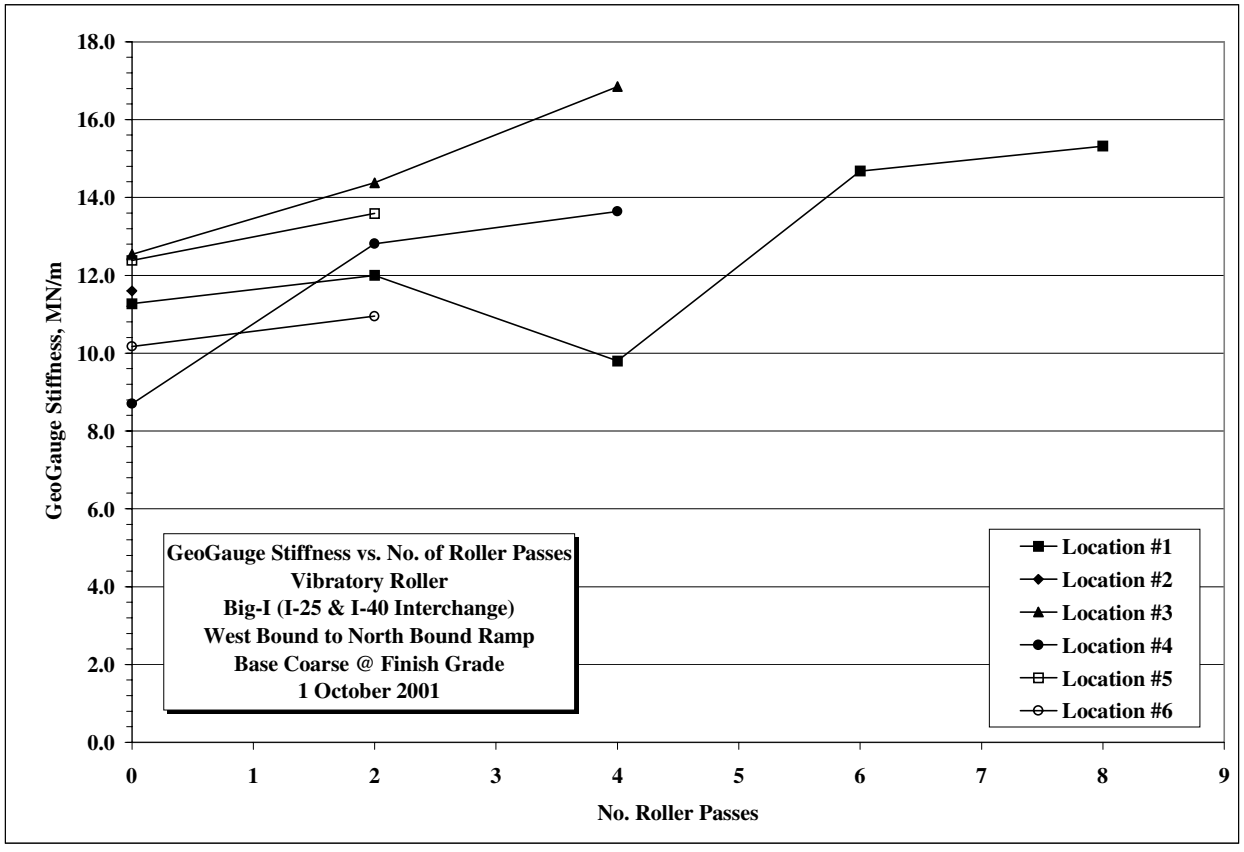

Figure 26. GeoGauge vs. Roller Passes, Base Course Material.

Figure 27. Field Measurements on Lime Stabilized Subgrade.

Table 2. Field Stiffness of Lime Stabilized Materials

Stiffness Test Results Lime Stabilized Sandy Clay - NM State Highway 44 (U.S. 550)					
Stiffness (MN/m)					
Location (Sta.)	Age (day)	Mean	Std. Dev.	COV (%)	Dry Density (pcf)
4815*	0	11.9	1.7	14.1	102.3
5045	1	13.4	2.5	18.3	101.5
5045	2	15.5	2.6	16.9	101.5
5050	14	22.6	3.1	13.5	101.0

***Unstabilized**

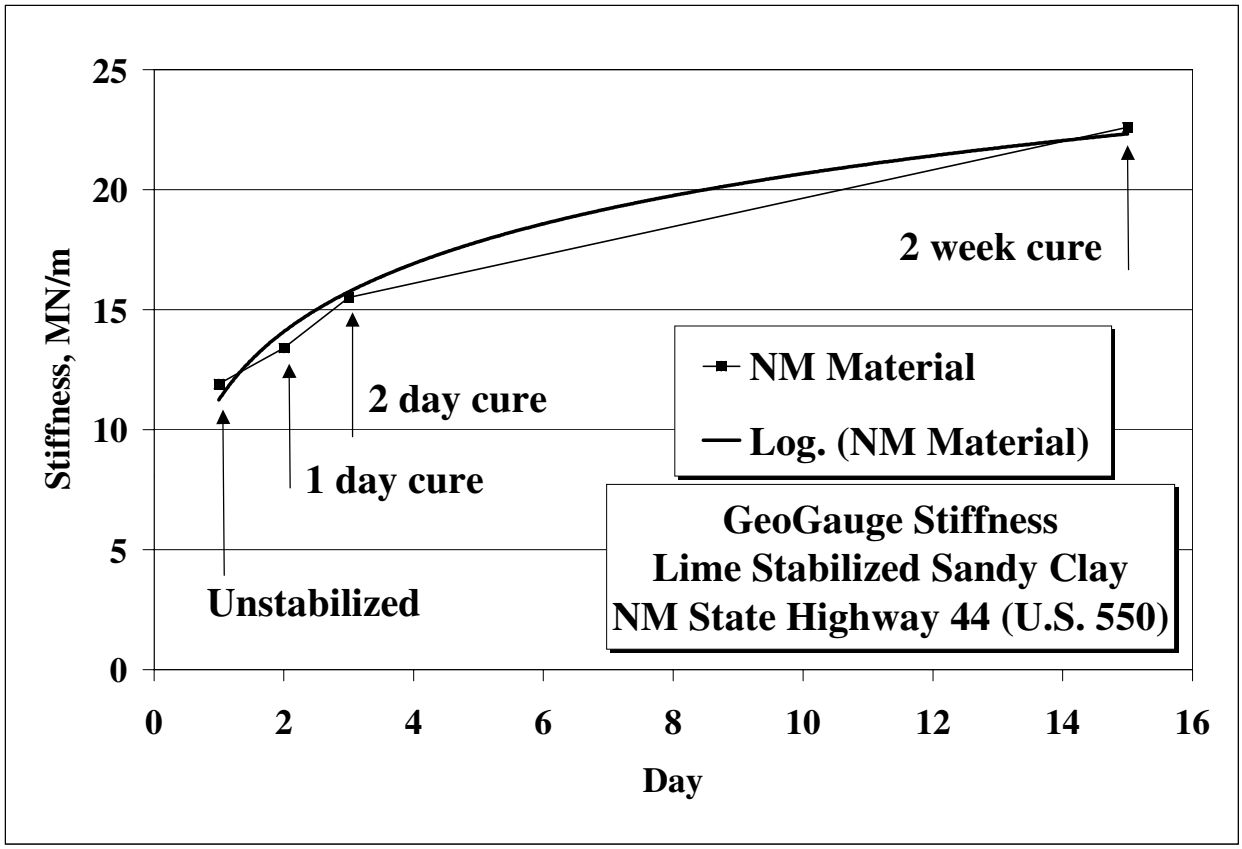

Figure 28. Field Stiffness vs. Time of Lime Stabilized Materials.

VII. CONCLUSIONS AND RECOMMENDATIONS

The Humboldt GeoGauge appears to have real potential as an alternative non-nuclear method for compaction control of highway materials. This study found that the GeoGauge does indeed measure soil stiffness as advertised. This was verified using classical theoretical and empirical soil mechanics concepts. Tests on cohesive soil showed that the soil stiffness does indeed vary with moisture content, consistent with concepts first shown by Turnbull and Foster and later by Seed and Chan. The optimum moisture for maximum stiffness does not in general coincide with the optimum moisture content for maximum density.

The quest for a laboratory method for determining a field target value for stiffness remains elusive, however. Attempts to ascertain a target value using modified Proctor molds were not successful because of boundary effects caused by the small volume of soil in relation to the size of the GeoGauge annular foot.

Field tests clearly show that stiffness increases can be observed with increasing compaction as evidenced by monitoring of roller passes. This is encouraging and suggests that implementation of the GeoGauge might be possible, albeit, with a substantial paradigm shift away from lab evaluation to appropriate field monitoring of compaction processes. Field tests also clearly show that stabilized materials evidence stiffness, and hence strength gains, over time. The GeoGauge can be a useful tool for monitoring such stiffness gains, but again the use of a priori laboratory stiffness data will be difficult, if not impossible, to develop for comparison purposes.

In the absence of a laboratory determined target value for stiffness in the field, future specifications, using GeoGauge like technology, may include careful control of moisture (still determined by the common Proctor test), along with well-defined field compaction procedures

and equipment. Such prescriptive specifications, along with monitoring of stiffness with the GeoGauge as compaction progresses, will result in maximum stiffness of subgrades, subbases, and base course materials at optimal moisture contents. The use of stiffness for control of compaction processes in the field, in contrast to current density control, will hopefully ensure superior, more uniform, and longer lasting pavement systems.

The use of a test strip, on a given project soil, to establish compaction control parameters using the GeoGauge may prove to be an acceptable alternative to the more conventional method of knowing the target value a priori. Such an approach would likely still require knowledge of moisture requirements (perhaps from the traditional Proctor test) and perhaps a specification of compaction equipment. However, compaction effort and rolling patterns would be determined in the field and GeoGauge stiffness determined corresponding to this established and agreed upon compactive effort. This GeoGauge stiffness value would then be the target, or specification value, for that soil for the duration of the project. Clearly, variability of the compaction process and the GeoGauge measurements would have to be considered in establishing this field specified stiffness.

VIII. REFERENCES

AASHTO T 99, *Standard Method of Test for Moisture-Density Relations of Soils Using a 5.5 lb (2.5 kg) Rammer and an 12 in. (305 mm) Drop*, Standard Specifications for Transportation Materials and Methods of Sampling and Testing, American Association of State Highway and Transportation Officials, Washington, DC, Part II, Tests.

AASHTO T 180, *Standard Method of Test for Moisture-Density Relations of Soils Using a 10 lb (4.54 kg) Rammer and an 18 in. (457 mm) Drop*, Standard Specifications for Transportation Materials and Methods of Sampling and Testing, American Association of State Highway and Transportation Officials, Washington, DC, Part II, Tests.

AASHTO T 191, *Standard Method of Test for Density of Soil In-Place by the Sand-Cone Method*, Standard Specifications for Transportation Materials and Methods of Sampling and Testing, American Association of State Highway and Transportation Officials, Washington, DC, Part II, Tests.

AASHTO T 205, *Standard Method of Test for Density of Soil In-Place by the Rubber-Balloon Method*, Standard Specifications for Transportation Materials and Methods of Sampling and Testing, American Association of State Highway and Transportation Officials, Washington, DC, Part II, Tests.

AASHTO T 238, *Standard Method of Test for Density of Soil and Soil-Aggregate in Place by Nuclear Methods (Shallow Depth)*, Standard Specifications for Transportation Materials and Methods of Sampling and Testing, American Association of State Highway and Transportation Officials, Washington, DC, Part II, Tests.

AASHTO T 239, *Standard Method of Test for Moisture Content of Soil and Soil-Aggregate in Place by Nuclear Methods (Shallow Depth)*, Standard Specifications for Transportation Materials and Methods of Sampling and Testing, American Association of State Highway and Transportation Officials, Washington, DC, Part II, Tests.

ASTM C 597, *Standard Test Method for Pulse Velocity Through Concrete,* Annual Book of ASTM Standards, American Society for Testing and Materials, West Conshohocken, PA, Vol. 4.02.

ASTM D 698, *Standard Test Method for Laboratory Compaction Characteristics of Soil Using Standard Effort (12,400 ft•lb/ft^3 (600 kN•m/m^3)),* Annual Book of ASTM Standards, American Society for Testing and Materials, West Conshohocken, PA, Vol. 4.08.

ASTM D 1556, *Standard Test Method for Density and Unit Weight of Soil in Place by the Sand-Cone Method*, Annual Book of ASTM Standards, American Society for Testing and Materials, West Conshohocken, PA, Vol. 4.08.

ASTM D 1557, *Standard Test Method for Laboratory Compaction Characteristics of Soil Using Modified Effort (56,000 ft•lb/ft^3 (2,700 kN•m/m^3)),* Annual Book of ASTM Standards, American Society for Testing and Materials, West Conshohocken, PA, Vol. 4.08.

ASTM D 2167, *Standard Test Method for Density and Unit Weight of Soil in Place by the Rubber Balloon Method*, Annual Book of ASTM Standards, American Society for Testing and Materials, West Conshohocken, PA, Vol. 4.08.

ASTM D 2922, *Standard Test Methods for Density of Soil and Soil-Aggregate in Place by Nuclear Methods (Shallow Depth)*, Annual Book of ASTM Standards, American Society for Testing and Materials, West Conshohocken, PA, Vol. 4.08.

ASTM D 3017, *Standard Test Method for Water Content of Soil and Rock in Place by Nuclear Methods (Shallow Depth)*, Annual Book of ASTM Standards, American Society for Testing and Materials, West Conshohocken, PA, Vol. 4.08.

Bendat, J.S., and Piersol, A.G., *Random Data: Analysis and Measurement Procedures*, 2nd Edit., John Wiley and Sons, New York, 1986, p. 30.

Egorov, K.E., *Calculation of Bed for Foundation with Ring Footing*, Proc. 6th International Conference of Soil Mechanics and Foundation Engineering, Vol. 2, 1965, pp. 41-45.

Hardin, B.O., and Richart, F.E., Jr., *Elastic Wave Velocities in Granular Soils*, Journal of the Soil Mechanics and Foundation Engineering Division, American Society of Civil Engineers, Vol. 89, No. SM1, 1963, pp. 33-65.

Holtz, R.D., and Kovacs, W.D., *An Introduction to Geotechnical Engineering*, Prentice-Hall, Englewood Cliffs, New Jersey, 1981.

Jaky, J., *The Coefficient of Earth Pressure at Rest*, Journal of the Union of Hungarian Engineers and Architects, 1944, pp. 355-358 (in Hungarian).

Kolsky, H., *Stress Waves in Solids*, Clarendon Press, Oxford, 1953 (Dover, New York, 1963).

Lenke, L.R., Pak, R.Y.S., and Ko, H-Y, *Boundary Effects in Modeling Foundations Subjected to Vertical Excitation*, Proc. International Conference Centrifuge 1991, Balkema, Rotterdam, 1991, pp. 473-480.

Poulos, H.G., and Davis, E.H., *Elastic Solutions for Soil and Rock Mechanics*, Wiley, New York, 1974, p. 32.

Turnbull, W.J., and Foster, C.R., *Stabilization of Materials by Compaction*, Journal of the Soil Mechanics and Foundations Division, American Society of Civil Engineers, Vol. 82, No. SM2, 1956, pp. 934-1 to 934-23.

Turnbull, W.J., and McRae, J.L., Soil Test Results Shown Graphically, Engineering News-Record, Vol. 144, 1950, pp. 38-39.

Seed, H.B., and Chan, C.K., *Structure and Strength Characteristics of Compacted Clays*, Journal of the Soil Mechanics and Foundations Division, American Society of Civil Engineers, Vol. 85, No. SM5, 1959, pp. 87-128.

Wood, D.M., *Soil Behaviour and Critical State Soil Mechanics*, Cambridge University Press, 1990.

THIS PAGE INTENTIONALLY LEFT BLANK